Thermochemistry and Electronic Structure of Small Boron and Boron Oxide Clusters and Their Anions

Minh Tho Nguyen,[†,‡] Myrna H. Matus,[†,§] Vu Thi Ngan,[‡] Daniel J. Grant,[†] and David A. Dixon*[,†]

Department of Chemistry, The University of Alabama, Shelby Hall, Tuscaloosa, Alabama 35487-0336, Department of Chemistry, University of Leuven, B-3001 Leuven, Belgium, and Unidad de Servicios de Apoyo en Resolución Analítica, Universidad Veracruzana, A. P. 575, Xalapa, Ver., Mexico

Received: December 24, 2008; Revised Manuscript Received: February 8, 2009

Thermochemical properties of a set of small boron (B_n) and boron oxide (B_nO_m) clusters, with $n = 1-4$ and $m = 0-3$, their anions, and the B_4^{2-} dianion, were calculated by using coupled-cluster theory CCSD(T) calculations with the aug-cc-pV*n*Z (n = D, T, Q, 5) basis sets extrapolated to the complete basis set limit with additional corrections. Enthalpies of formation, bond dissociation energies, singlet−triplet or doublet−quartet separation gaps, adiabatic electron affinities (EA), and both vertical electron attachment and detachment energies were evaluated. The predicted heats of formation show agreement close to the error bars of the literature results for boron oxides with the largest error for OBO. Our calculated adiabatic EAs are in good agreement with recent experiments: B (calc, 0.26 eV; exptl, 0.28 eV), B_2 (1.95, 1.80), B_3 (2.88, 2.820 ± 0.020), B_4 (1.68, 1.60 ± 0.10), BO (2.50, 2.51), BO_2 (4.48, 4.51), BOB (0.07), B_2O_2 (0.37), B_3O (2.05), B_3O_2 (2.94, 2.94), B_4O (2.58), and B_4O_2 (3.14, 3.160 ± 0.015). The BO bond is strong, so this moiety is maintained in most of the clusters. Thermochemical parameters of clusters are not linearly additive with respect to the number of B atoms. The EA tends to be larger in the dioxides. The growth mechanism of small boron oxides should be determined by a number of factors: (i) formation of BO bonds, (ii) when possible, formation of a cyclic B_3 or B_4, and (iii) combination of a boron cycle and a BO bond. When these factors compete, the strength of the BO bonds tends to compensate the destabilization arising from a loss of binding in the cyclic boron clusters, in such a way that a linear boron oxide prevails. When the B_2 moiety is present in these linear clusters, the oxide derivatives prefer a high spin state.

Introduction

Boron has a rich chemistry, which has been extensively studied.[1−3] Elemental boron has high volumetric and gravimetric heats of combustion; the heat of combustion of boron hydrides is typically ∼30 000 BTUs/lb, whereas the value of a hydrocarbon fuel such as kerosene is ∼18 500 BTUs/lb (43.1 MJ/kg). Thus, boron derivatives have long been used as additives in high energy density fuels, propellants, and explosives.[4] Because of their low molecular weights and polar B−H bonds, boron hydrides are currently being considered in combination with other hydrides for the development of materials for chemical hydrogen storage for the transportation sector.[5] Intensive studies of borane amine (BH_3NH_3) and its derivatives have been made for onboard hydrogen storage in the transportation sector.[6] In high temperature systems, the decomposition of boron compounds can lead to the formation of boron clusters (B_n) as intermediates, which may readily react with oxygen to form boron oxides (B_nO_m). Indeed, naturally occurring boron is usually found as a borate.

Boron clusters have been the subject of extensive theoretical and experimental studies, and comprehensive reviews[7,8] on the molecular structures and spectroscopic properties of boron clusters ranging from small aggregates to nanotubes are available. For example, recent computational studies predict that the boron buckyball B_{80} has an electronic structure similar to that of the carbon C_{60}.[9] Previous experimental studies on small boron oxides include mass spectrometry,[10,11] and microwave,[12] infrared,[13−15] electronic,[16−20] and photoelectron[21−23] spectroscopy techniques. For example, Anderson and co-workers[11] used mass spectrometry to investigate the oxidation of boron clusters and the subsequent reactions of the $B_nO_m^+$ cations with small molecules such as HF and H_2O. Most of the available quantum chemical studies on boron oxides are for clusters containing up to three boron atoms.[24−39] For example, Drummond et al.[39] investigated the molecular structure and stability of a larger set of B_nO_m compounds, with $m = 1-3$ and $n = 1-7$, using molecular dynamics techniques in conjunction with plane-wave periodic density functional theory (DFT). Both gas-phase and solid bulk structures were considered. Wang and cowokers[23c] studied anions and dianions of the B_4O_2 system using photoelectron spectroscopy and electronic structure calculations to predict the occurrence of boron−boron triple bond character. Comparison with the structure of pure boron clusters indicated considerable structural changes upon addition of oxygen atoms.[39] There have been extensive discussions of the resonance structures of the comparable Al_x^- clusters, and the concept of 3-fold aromaticity has been introduced to explain the bonding and energetic of Al_x^- structures.[40]

We have significant efforts underway to predict accurately the thermochemistry of different classes of boron hydride derivatives and to probe the molecular mechanisms of their H_2 release processes.[41−43] As part of work in the overall chemistry

* Corresponding author. E-mail: dadixon@bama.ua.edu.
† The University of Alabama.
‡ University of Leuven.
§ Universidad Veracruzana.

10.1021/jp811391v CCC: $40.75
Published on Web 03/30/2009

of these boron compounds, we have predicted the heats of formation and electronic structure of a set of small boron oxides, using the same high accuracy computational methods. We studied the neutral B_nO_m compounds, with $n = 1-4$ and $m = 0-3$, and their negatively charged derivatives.

Computational Methods

Electronic structure calculations were carried out by using the Gaussian 03[44] and MOLPRO[45] suites of programs. Enthalpies of formation of the stationary points were calculated from the corresponding total atomization energy (TAE).[46] We first calculated the valence electronic energies using coupled-cluster (CCSD(T)) theory[47] extrapolated to the complete basis set limit (CBS) using the correlation-consistent basis sets.[48] Geometry parameters were fully optimized at the CCSD(T) level with the correlation consistent aug-cc-pVDZ and aug-cc-pVTZ basis sets. The fully unrestricted formalism (UHF, UCCSD) was used for open-shell system calculations done with Gaussian 03. The single-point electronic energies were calculated by using the restricted coupled-cluster R/UCCSD(T) formalism[49-51] in conjunction with the correlation-consistent aug-cc-pV*n*Z (n = D, T, and Q) basis sets at the (U)CCSD(T)/aug-cc-pVDZ or (U)CCSD(T)/aug-cc-pVTZ optimized geometries. For simplicity, the basis sets are denoted hereafter as aV*n*Z. The individual valence CCSD(T) energies, $E(n)$, for a given basis set were extrapolated to the CBS limit energy, E_{CBS}, by using the mixed exponential/Gaussian function (eq 1):[52]

$$E(n) = E_{CBS} + A \exp[-(n-1)] + B \exp[-(n-1)^2] \quad (1)$$

with $n = 2$ (aVDZ), 3 (aVTZ), and 4 (aVQZ), respectively, and A and B are fitting parameters. The total atomization energies for the smaller molecules where the aV5Z basis set could be used were also obtained by extrapolating the aVQZ and aV5Z energies using the expression:[53]

$$E(l_{max}) = E_{CBS} + B/l_{max}^3 \quad (2)$$

where $l_{max} = 4$ and 5 for the aVQZ and aV5Z basis sets, respectively, and B is a fitting parameter. The quantity l_{max} is the highest angular momentum value in the basis set (g functions for aVQZ and h functions for aV5Z). Total CCSD(T) electronic energies as a function of basis set are given in Table S1 of the Supporting Information.

After the valence electronic energy, the largest contribution to the TAE is the zero-point energy (ZPE). For the diatomic species, harmonic frequencies and anharmonic constants were calculated from a fifth-order fit[54] of the potential energy curves at the CCSD(T)/aVQZ level. Harmonic vibrational frequencies of the polyatomics were calculated at the CCSD(T)/aVDZ or CCSD(T)/aVTZ levels of calculation for BO_m, B_2O_m ($m = 1$, 2), and B_2O_3 systems, and at the MP2/aVDZ, MP2/aVTZ, or CCSD(T)/aVDZ levels of calculation for B_nO_m ($n = 3$, 4; $m = 0$, 1, and 2) systems (see Table S2 of the Supporting Information for further details).

Additional smaller corrections were included in the TAE calculations. Core-valence corrections (ΔE_{CV}) were obtained at the CCSD(T)/cc-pwCVTZ level of theory.[55] Douglas−Kroll−Hess (DKH) scalar relativistic corrections ($\Delta E_{DKH\text{-}SR}$), which account for changes in the relativistic contributions to the total energies of the molecule and the constituent atoms, were calculated using the spin-free, one-electron DKH Hamiltonian.[56-58] $\Delta E_{DKH\text{-}SR}$ is defined as the difference in the atomization energy between the results obtained from basis sets recontracted for DKH calculations[57] and the atomization energy obtained with the normal valence basis set of the same quality. Thus, DKH calculations were carried out at the CCSD(T)/cc-pVTZ and the CCSD(T)/cc-pVTZ-DK levels of theory. Most calculations using available electronic structure computer codes do not correctly describe the lowest energy spin multiplet of an atomic state as spin−orbit in the atom is usually not included. Instead, the energy is a weighted average of the available multiplets. The spin−orbit corrections are 0.03 kcal/mol for B and 0.223 kcal/mol for O, both from the excitation energies of Moore.[59]

The total atomization energy ($\sum D_0$ or TAE) of a compound is given by the expression:

$$\sum D_0 = \Delta E_{elec}(CBS) + \Delta E_{CV} + \Delta E_{DKH\text{-}SR} + \Delta E_{SO} - \Delta E_{ZPE} \quad (3)$$

By combining our computed $\sum D_0$ values with the known heats of formation at 0 K for the elements ($\Delta H_f°(B) = 135.1 \pm 0.2$ kcal/mol,[60] and $\Delta H_f°(O) = 58.98 \pm 0.02$ kcal/mol[61]), we can derive $\Delta H_f°$ values at 0 K for the molecules in the gas phase. The heat of formation of the boron atom has changed over time. The original JANAF value[61] was $\Delta H_f°(0\ K, B) = 132.7 \pm 2.9$ kcal/mol. Storms and Mueller[62] recommended a much larger value of 136.2 ± 0.2 kcal/mol, which based on the analysis of Ruscic and co-workers[63] we used in our previous work.[41-43] Martin and Taylor[64] calculated the atomization energies of BF and BF_3 by using a composite approach based on CCSD(T), used these results to predict the heat of formation of the boron atom, and came to a similar conclusion as that of Ruscic.[63] More recently, Karton and Martin[60] revised the heat of formation of the B atom to 135.1 ± 0.2 kcal/mol on the basis of the experimental heats of formation of BF_3[65] and B_2H_6[66] coupled with W4 calculations of their total atomization energies, and this is the value we have used. We obtain heats of formation at 298 K by following the procedures outlined by Curtiss et al.[67]

The vertical electron attachment energy (VAE, attachment of an electron at the neutral geometry) and electron detachment energy (VDE, detachment of an electron at the anion geometry) were computed at the CCSD(T)/aVQZ level using the CCSD(T)/aVTZ optimized geometries of the neutrals (for VAE) and anions (for VDE). The adiabatic electron affinity (EA) is obtained as the energy difference between the neutral at its optimum geometry and the anion at its optimum geometry.

Results and Discussion

Comparisons of experimental and calculated values of geometry parameters and vibrational modes are shown in Tables 1 and 2, respectively. The different components used to predict the total atomization energies ($\sum D_0$) and the $\sum D_0$ are given in Table 3. The predicted enthalpies of formation at 0 and 298 K are summarized in Table 4, together with the available experimental values. Heats for a variety of reactions involving boron and boron oxide clusters are recorded in Table 5. The EAs, VAEs, and VDEs are given in Tables 6 and 7, and the EAs as a function of basis set are given in Table S3 of the Supporting Information.

Boron Clusters (B_2, B_3, and B_4) and Their Anions. To predict the oxidation reactions of the boron clusters, reliable energetics for these species are needed; however, the thermochemical parameters of boron clusters have not been extensively

TABLE 1: Comparison of Geometrical Parameters (Distances in Å and Angles in deg) for Selected B_nO_m Compounds

structure	level	parameter	this work	expt.
B_2 ($^3\Sigma_g^-$)	CCSD(T)/aVQZ	d(B−B)	1.5940	1.590[a]
B_3 ($^2A_1'$)	CCSD(T)/aVTZ	d(B−B)	1.570	1.6038
BO ($^2\Sigma^+$)	CCSD(T)/aVQZ	d(B−O)	1.2094	1.2045[a]
BO ($^2\Pi$)	CCSD(T)/aVQZ	d(B−O)	1.3600	1.353[a]
BO^-($^1\Sigma$)	CCSD(T)/aVQZ	d(B−O)	1.2413	1.236 ± 0.010[b]
OBO ($^2\Pi$)	CCSD(T)/aVTZ	d(B−O)	1.2716	1.265 ± 0.002[c] 1.26485(5)[d]
OBOBO ($^1A_1$)	CCSD(T)/aVDZ	d(B═O)	1.2227	1.195(6)[d]
		d(B−O)	1.3476	1.329(10)[d]
		∠(B−O−B)	133.0	134.2(50)[d]
		∠(O═B−O)	177.2	173.4(44)[d]

[a] Reference 72. [b] Reference 22. [c] Reference 106. [d] Reference 107.

TABLE 2: Comparison of Calculated and Experimental Vibrational Modes (cm^{-1}) for Some B_nO_m ($n = 1-4$, $m = 0-3$) Compounds

structure	symmetry	this work	expt.
B_2 ($^3\Sigma_g^-$)[a]	ω_e	1047.1	1051.3[b]
	$\omega_e\chi_e$	9.1	9.35[b]
BO ($^2\Sigma^+$)[a]	ω_e	1873.8	1885.69[b]
	$\omega_e\chi_e$	11.7	11.81[b]
BO ($A^2\Pi$)[a]	ω_e	1250.7	1260.701[b]
	$\omega_e\chi_e$	11.0	11.157[b]
BO ($^1\Sigma^+$)[a]	ω_e	1707.0	1665 ± 30[c]
	$\omega_e\chi_e$	11.3	
OBO ($^2\Pi_g$)[d]	σ_g	1095.1	1056.4[e]
	σ_u	1054.8	1278.3[f]
	π_u	446.4[o]	448.2[g]
BO_2^- ($^1\Sigma_g^+$)[d]	σ_u	1932.1	1931[h]
	σ_g	1076.3	
	π_u	583.4	587.8[h]
BOB ($^1A_1 = {}^1\Sigma_g^+$)[i]	b_2	1449.7	1415.7[h]
	a_1	1047.7	
	a_1	62.0	
OBBO ($^1\Sigma_g^+$)[j]	σ_g	2051.6	
	σ_u	1865.3	1898.9,[h,k] 1894.6[h,k]
	σ_g	603.0	
	π_g	497.3	
	π_u	212.9	213.0[i,k]
OBOBO ($^1A_1$)[j]	a_1	2033.8	2062.0[h]
	b_2	2030.6	
	b_2	1162.7	
	a_1	744.0	
	a_1	548.8	
	b_1	494.5	
	a_2	473.5	
	b_2	458.2	
	a_1	106.4	
B_3 ($^2A_1'$)[j]	a_1'	1185.8	1020 ± 50[l]
	e'	890.6	886.2[m]
OBBBO	b_2	1954	1950 ± 40[n]
	a_1	1935	

[a] Fit at the CCSD(T)/aVQZ level of calculation. [b] Reference 72. [c] Reference 22. [d] CCSD(T)/aVTZ. [e] Reference 108. [f] Reference 109. [g] Reference 20. [h] Reference 13. [i] At the CCSD(T) level, BOB has a C_{2v} bent r_e structure ($^1A_1$) but a linear r_o form ($^1\Sigma_g^+$). [j] CCSD(T)/aVDZ. [k] Reference 117. [l] Reference 81. [m] Reference 80. [n] Reference 23. [o] Obtained as an average of two π frequencies of 487.6 and 405.1 cm^{-1}.

studied computationally[7,28] or experimentally. We calculated the structures and energies of the corresponding anions to obtain electron affinities, and included the tetramer dianion B_4^{2-}. For each species, both low and high spin electronic states were studied. Unless otherwise noted, geometry parameters refer to the (U)CCSD(T)/aVTZ optimized values.

B_2. The calculated distance for the gaseous diatomic B_2 ($^3\Sigma_g^-$) is in excellent agreement with the experimental value.[68] Our calculated bond energy for B_2 is close to the G1 value[69,70] and the value obtained by using multireference configuration interaction calculations (MRCI) with a large ANO basis set.[71] The theoretical values are consistently smaller by ~0.2 eV than the Huber and Herzberg[72] or that from Gurvich et al. values,[66] which are from a mass spectrometric study.[73] The first excited state of B_2 is the high spin $^5\Sigma_u^-$ state, and it is calculated to be 3.4 kcal/mol above the ground state. Previous MRCI calculations predicted a value of 5.0 kcal/mol for the quintet−triplet gap.[74] The $^1\Sigma_g^+ - {}^3\Sigma_g^-$ gap to the first excited singlet state is 15.6 kcal/mol (Table 4).

Attachment of one electron to B_2 ($^3\Sigma_g^-$) to form the low spin $^2\Pi_u$ anion shortens the bond distance, but formation of the high spin $^4\Sigma_g^-$ anion leads to a longer bond length. In agreement with earlier studies,[7] we predict that the $^4\Sigma_g^-$ state is the ground state of B_2^- with a doublet−quartet gap of 11.6 kcal/mol. The EA from mass spectrometric studies[75] is too small as compared to the calculated EA (Table 6). Calculations at the MP4SDQ/CBSB5 level[76] led to a value that is clearly incorrect. The current NIST database[77] estimate is close to our predicted value. Although there is an increase in the B−B bond distance in the anion, the difference between both VAE and VDE is small (Table 7). The dimer has a substantially larger electron affinity than does the atom.[78]

B_3. The boron trimer and its anion have extensively been studied both experimentally and theoretically.[7] The SOMO ($2a_1'$) of B_3 in D_{3h} symmetry is a σ-orbital so the radical is not subject to a Jahn−Teller distortion in the $^2A_1'$ ground state. The calculated B−B bond distance is shorter by 0.034 Å from one indirectly derived from an electronic spectroscopic study.[79] For B_3, the TAEs of 189.1[64] and 185.0[7] kcal/mol at a modified G1 level and the CCSD(T)/6-311+G(2df) level, respectively, are significantly smaller than the present CBS value (Table 5). Formation of B_3 from B_2 + B is exothermic by −130.9 kcal/mol. For comparison, the binding energy of the Al atom to Al_2 is 54.4 kcal/mol at the same CCSD(T)/CBS level.[40] The calculated value for the e′ mode is in excellent agreement with experiment,[80] but there is a substantial difference between the calculated and experimental[81] values for the a_1' mode. The T_1 diagnostic[82] for B_3 is 0.021, which suggests that there could be a modest amount of multireference character but not a large amount.

The B_3 radical has a doublet ground state, and there are a number of low-lying excited states in the doublet manifold.[83] In the high spin quartet manifold, the $^4A_2$ state has the lowest energy, with an adiabatic doublet−quartet separation energy of 35.2 kcal/mol. The B_3^- anion is a ground-state D_{3h} triplet. Photoelectron spectroscopy studies of the B_3^- anion determined the vertical position of the lowest doublet and quartet states of

TABLE 3: Components for the Atomization Energies and Thermal Corrections (TC) for B_nO_m ($n = 1-4$, $m = 0-3$) Compounds in kcal/mol

structure	ΔE_{CBS} (DTQ) [ΔE_{CBS} (Q5)]	ΔE_{DKH-SR}	ΔE_{CV}	ΔE_{SO}	ΔE_{ZPE}	$\sum D_0$ (DTQ) [$\sum D_0$ (Q5)]	TC
B^- (^3P)	5.79 [5.93]	−0.03	0.22	−0.03		5.94 [6.08]	1.48
B_2 ($^3\Sigma_g^-$)	65.29 [65.29]	−0.06	0.66	−0.06	1.49	64.35 [64.34]	2.09
B_2 ($^1\Sigma_g^+$)	49.59 [48.94]	−0.06	0.57	−0.06	1.38	48.66 [48.00]	2.10
B_2 ($^5\Sigma_u^-$)	61.64 [61.59]	−0.13	1.28	−0.06	1.80	60.93 [60.87]	2.08
B_2^- ($^2\Pi_u$)	98.41 [98.52]	−0.09	0.94	−0.06	1.54	97.66 [97.76]	2.09
B_2^- ($^4\Sigma_g^-$)	109.84 [109.93]	−0.08	1.00	−0.06	1.42	109.28 [109.37]	2.09
BO ($^2\Sigma^+$)	194.35 [194.16]	−0.23	1.21	−0.25	2.67	192.41 [192.22]	2.07
BO ($^2\Pi$)	126.33 [126.33]	−0.11	0.46	−0.25	1.78	124.64 [124.64]	2.08
BO^- ($^1\Sigma^+$)	251.89 [251.83]	−0.25	1.19	−0.25	2.43	250.15 [250.09]	2.08
OBO ($^2\Pi_g$)	322.12	−0.37	1.78	−0.48	3.98[a]	319.07	2.45
OBO ($^4B_1$)	220.74	−0.26	1.20	−0.48	3.97	217.23	2.56
BOO ($^2A'$)	180.86	−0.26	0.56	−0.48	3.51	177.17	2.72
BO_2^- ($^1\Sigma_g^+$)	427.55	−0.55	1.92	−0.48	5.97	422.46	2.30
BBO ($^1\Sigma^+$)	275.24	−0.24	1.61	−0.28	4.34	271.98	2.80
BBO ($^3\Pi$)	259.37	−0.36	2.04	−0.28	4.85	255.93	2.57
BOB ($^1\Sigma_g^+$)	291.43	−0.28	1.11	−0.28	3.66	288.31	2.45
BOB ($^3\Pi_u$)	224.64	−0.30	1.40	−0.28	3.49	221.97	2.84
BOB ($^3B_2$)	252.12	−0.31	1.85	−0.28	4.46	248.91	2.90
BOB^- ($^2\Sigma_g^+$)	291.95	−0.33	1.43	−0.28	2.76	290.00	2.91
OBBO ($^1\Sigma_g^+$)	504.32	−0.47	3.16	−0.51	8.50	498.01	3.14
OBBO ($^3\Pi_u$)	425.88	−0.62	2.39	−0.51	7.33	419.81	2.82
BOBO ($^1A'$)	475.25	−0.55	2.26	−0.51	7.53	468.92	3.14
BOBO ($^3A'$)	402.18	−0.63	2.64	−0.51	7.54	396.13	3.08
$OBBO^-$ (^2B_u)	511.29	−0.57	2.94	−0.51	6.61	506.54	3.45
OBOBO ($^1A_1$)	654.87	−0.84	3.51	−0.73	11.52	645.29	3.47
B_3 ($^2A_1'$)	197.40	−0.15	2.29	−0.09	4.24	195.21	2.45
B_3 ($^4A_2$)	161.68	−0.15	1.94	−0.09	3.41	159.98	2.60
B_3^- ($^1A_1'$)	263.50	−0.18	2.69	−0.09	4.34	261.58	2.44
B_3^- ($^3B_2$)	228.75	−0.18	2.47	−0.09	3.69	227.26	2.53
BBBO ($^4\Sigma^-$)	371.12	−0.35	3.12	−0.31	7.24	366.33	3.30
BBOB ($^4A''$)	344.85	−0.43	2.52	−0.31	6.34	340.28	2.87
B_3O^- ($^1\Sigma_g^+$)	384.73	−0.42	3.23	−0.31	7.53	379.70	3.18
B_3O^- ($^3A''$)	418.41	−0.39	2.96	−0.31	6.95	413.71	3.15
B_3OO ($^2A_1$)	363.96	−0.33	1.85	−0.54	7.71	357.22	3.52
B_3OO ($^2B_1$)	390.52	−0.38	2.18	−0.54	7.87	383.91	3.90
OB_3O ($^2\Pi_u$)	569.13	−0.54	4.04	−0.54	10.01	562.10	3.38
OB_3O ($^4\Pi_u$)	471.71	−0.49	3.41	−0.54	10.77	463.32	4.04
$B_3O_2^-$ ($^1A_1$)	621.84	−0.60	3.87	−0.54	9.76	614.80	3.80
$B_3O_2^-$ ($^3\Sigma_g^-$)	639.94	−0.62	4.15	−0.54	10.15	629.78	3.98
B_4 (^1A_g)	319.70	−0.28	3.67	−0.12	7.16	315.82	2.98
B_4 ($^3B_{1u}$)	282.88	−0.25	3.90	−0.12	8.71	277.71	2.68
B_4^- ($^2B_{1u}$)	357.82	−0.25	3.98	−0.12	6.86	354.57	2.86
B_4^{2-} (^1A_g)	293.71	−0.34	3.69	−0.12	6.18	290.75	2.95
B_4^{2-} ($^1A_{1g}$)	284.87	−0.21	3.12	−0.12	5.36	282.28	3.17
BBBBO(**A**,$^1\Sigma^+$)[b]	429.09	−0.43	3.85	−0.34	9.51	422.65	4.15
BBBBO (**A**, $^3\Pi$)[b]	458.10	−0.37	3.87	−0.34	9.55	451.72	4.10
B_4O (**C**, $^1A'$)[b]	492.66	−0.50	4.12	−0.34	10.57	485.37	3.18
B_4O (**C**, $^3A'$)[b]	455.47	−0.51	3.94	−0.34	10.03	448.53	3.30
B_4O (**D**, $^1A_1$)[b]	493.30	−0.41	3.87	−0.34	9.76	486.65	3.70
B_4O^- (**D**,$^2A_1$)[b]	554.20	−0.47	4.22	−0.34	11.53	546.07	3.58
OBBBBO ($^1\Sigma_g^+$)	660.85	−0.61	4.77	−0.57	12.53	651.91	4.72
OBBBBO ($^3\Sigma_g^-$)	675.38	−0.61	4.86	−0.57	12.64	666.43	4.71
$B_4O_2^-$ ($^2\Pi_u$)	747.62	−0.73	5.00	−0.57	12.52	738.79	4.65

[a] Taken from experimental values. [b] See Figure 5 for definition of structures **A**, **C**, and **D**.

the neutral trimer[84] to be separated by 39.9 kcal/mol (1.73 eV) in comparison with our calculated value of 35.2 kcal/mol.

In the B_3^- anion, the additional electron is added to the doublet B_3 in the σ-orbital $2a_1'$, to form a closed-shell $^1A_1'$ (D_{3h}) ground state with a small decrease in the B−B distance. The lowest lying triplet state of B_3^- distorts to the C_{2v} $^3B_2$ state with a slightly shorter B−B distance. The singlet−triplet gap in B_3^- is 34.3 kcal/mol, comparable to the doublet−quartet gap in B_3. The Jahn−Teller effects accompanying the photodetachment of B_3^- have been analyzed in detail.[85] The calculated VDE is in excellent agreement with the photoelectron spectroscopy[84] VDE. The VAE and VDE are essentially the same. We note that the adiabatic EAs are determined from the calculated CCSD(T)/CBS heats of formation, and the VDEs were calculated using only the CCSD(T)/aVQZ energies. Previous MP4SDQ/CBS calculations[76] predict a value of 3.20 eV for EA(B_3) that is again too large. Relative to the dimer, the boron trimer EA increases by 0.85 eV.

The chemical bonding in boron clusters has been probed using a variety of theoretical methods.[86] We present in Figure 1 an additional way to describe the electron distribution of the B_3 clusters using the electron localization function (ELF) approach.[87,88] The electron density in the trimer is equally partitioned, presumably due to its high symmetry, with ∼2 electrons in each

TABLE 4: Heats of Formation for B_nO_m ($n = 1-4$, $m = 0-3$) Compounds in kcal/mol

structure	$\Delta H_{f,0K}$ (DTQ) [(Q5)]	$\Delta H_{f,298K}$ (DTQ) [(Q5)]	$\Delta H_{f,298K}$ (exptl)[a]
B^- (^3P)	129.2 [129.0]	130.3 [130.2]	128.6 ± 2.7
B_2 ($^3\Sigma_g^-$)	205.9 [205.9]	207.4 [207.4]	198.3 ± 8.0
B_2 ($^1\Sigma_g^+$)	221.5 [222.2]	223.1 [223.7]	
B_2 ($^5\Sigma_u$)	209.3 [209.3]	210.8 [210.8]	
B_2^- ($^2\Pi_u$)	172.5 [172.4]	174.1 [173.9]	
B_2^- ($^4\Sigma_g^-$)	160.9 [160.8]	162.4 [162.3]	168.5 ± 9.2[b]
BO ($^2\Sigma^+$)	1.7 [1.9]	2.4 [2.6]	0.0 ± 2.0
BO ($^2\Pi$)	69.4 [69.4]	70.2 [70.2]	
BO^- ($^1\Sigma^+$)	−56.1 [−56.0]	−55.3 [−55.3]	
OBO ($^2\Pi_g$)	−66.0	−65.9	−68.1± 2.0, −69.8 ± 2.0
OBO ($^4B_1$)	35.8	36.0	
BOO ($^2A'$)	75.9	76.3	
BO_2^- ($^1\Sigma_g^+$)	−169.4	−169.5	−166.1 ± 6.0
BBO ($^1\Sigma^+$)	57.2	58.4	
BBO ($^3\Pi$)	73.3	74.2	
BOB ($^1\Sigma_g^+$)	40.9	41.7	22.9 ± 25.1
BOB ($^3\Pi_u$)	107.2	108.4	
BOB ($^3B_2$)	80.3	81.5	
BOB^- ($^2\Sigma_g^+$)	39.2	40.5	
OBBO ($^1\Sigma_g^+$)	−109.8	−109.4	−109.0 ± 2.0
OBBO ($^3\Pi_u$)	−31.6	−31.5	
BOBO ($^1A'$)	−80.8	−80.3	
BOBO ($^3A'$)	−8.0	−7.5	
$OBBO^-$ (^2B_u)	−118.4	−117.6	
OBOBO ($^1A_1$)	−198.1	−198.4	−199.8± 1.0
B_3 ($^2A_1'$)	210.1	211.7	
B_3 ($^4A_2$)	245.3	247.1	
B_3^- ($^1A_1'$)	143.7	145.3	
B_3^- ($^3B_2$)	178.0	179.7	
BBBO ($^4\Sigma^-$)	98.0	99.3	
BBOB ($^4A''$)	124.0	125.0	
B_3O^- ($^1\Sigma_g^+$)	84.6	85.8	
B_3O^- ($^3A''$)	50.6	51.8	
B_3OO ($^2A_1$)	166.0	166.6	
B_3OO ($^2B_1$)	139.3	140.3	
OB_3O ($^2\Pi_u$)	−38.8	−38.4	
OB_3O ($^4\Pi_u$)	59.9	61.0	
$B_3O_2^-$ ($^1A_1$)	−91.5	−90.7	
$B_3O_2^-$ ($^3\Sigma_g^-$)	−106.5	−105.5	
B_4 (^1A_g)	224.6	226.4	
B_4 ($^3B_{1u}$)	262.7	264.2	
B_4^- ($^2B_{1u}$)	185.8	187.5	
B_4^{2-} (^1A_g)	249.6	251.4	
B_4^{2-} ($^1A_{1g}$)	258.1	260.1	
BBBBO (**A**, $^1\Sigma^+$)[c]	176.7	178.7	
BBBBO (**A**, $^3\Pi$)[c]	147.7	149.6	
B_4O (**C**, $^1A'$)[c]	114.0	115.0	
B_4O (**C**, $^3A'$)[c]	150.9	151.9	
B_4O (**D**, $^1A_1$)[c]	112.7	114.2	
B_4O^- (**D**, $^2A_1$)[c]	53.3	54.7	
OBBBBO ($^1\Sigma_g^+$)	6.5	7.9	
OBBBBO ($^3\Sigma_g^-$)	−8.1	−6.6	
$B_4O_2^-$ ($^2\Pi_u$)	−80.4	−79.0	

[a] Taken from ref 61, unless otherwise noted. [b] Reference 75. [c] See Figure 5 for definition of structures **A**, **C**, and **D**.

of the three (BB) basins, and ∼1 electron in each of three nonbonding basins (Figure 1a).

The B_3^- orbitals are shown in Figure 2a. The HOMO is clearly composed of the three in-plane orbitals that point to the center of the ring just as in Al_4^{2-}. The NHOMO is the out-of-plane symmetric interaction of the B 2p orbitals. The NHOMO−2 is degenerate and is composed of s and p orbitals in the plane. The most stable valence orbital is composed predominantly of the bonding interaction of the 2s orbitals. This is significantly different from what is found in the analogous Al clusters due to the fact that the 3s orbitals in Al do not hybridize as well as the 2s orbitals in the B clusters.[40]

Using the Dewar resonance energy model,[89] following the approach used for $RE(Al_3^-)$ (eq 3),[40] and assuming aromaticity with one active electron from each B as in Al^{3-}, we obtain the following for $RE(B_3^-)$:

$$RE(B_3^-) = \Delta E(B_3^- \rightarrow 3B + e^-) - n\Delta E(B_2(^3\Sigma_g^-) \rightarrow 2B) \quad (4)$$

with $n = 2$. This gives RE = 133 kcal/mol, and it is even higher if we use the $^1\Sigma_g^+$ state for B_2. This RE is much larger than the values ranging between 65 and 79 kcal/mol for Al_3^-. The other limit would be to assume that there are three B−B bonds as our model nonaromatic system so that $n = 3$ in eq 4 and RE = 68 kcal/mol, which is more similar to the RE of Al_3^-. Even if the reactions shown above were to go to $2B + B^-$, this would

TABLE 5: Reaction Energies Taken from the Heats of Formation in kcal/mol

reaction	$\Delta H_{0K\text{-}DTQ}$ [$\Delta H_{0K\text{-}Q5}$]	$\Delta H_{298K\text{-}DTQ}$ [$\Delta H_{298K\text{-}Q5}$]
B (^{2}P) + O_2 ($^3\Sigma_g^-$) → BO ($^2\Sigma$) + O (^{3}P)	−74.5 [−74.3]	−73.1 [−72.9]
B_2 ($^3\Sigma_g^-$) + O_2 ($^3\Sigma_g^-$) → BBO ($^1\Sigma^+$) + O (^{3}P)	−89.7	−89.4
B_3 ($^2A_1'$) + O_2 ($^3\Sigma_g^-$) → BBBO ($^4\Sigma^-$) + O (^{3}P)	−53.2	−52.8
B_4 (^1A_g) + O_2 ($^3\Sigma_g^-$) → BBBBO ($^3\Sigma^-$) + O (^{3}P)	−17.9	−17.3
B_4 (^1A_g) + O_2 ($^3\Sigma_g^-$) → B_4O ($^1A'$) + O (^{3}P)	−51.6	−51.9
B_4 (^1A_g) + O_2 ($^3\Sigma_g^-$) → B_4O ($^1A_1$) + O (^{3}P)	−52.9	−52.6
BO ($^2\Sigma^+$) → B (^{2}P) + O (^{3}P)	192.4 [192.2]	192.2 [192.0]
BO ($^2\Sigma^+$) → BO ($^2\Pi$)	67.8 [67.6]	67.8 [67.6]
OBO ($^2\Pi_g$) → BO ($^2\Sigma^+$) + O (^{3}P)	126.7	127.9
OBO ($^2\Pi_g$) → B (^{2}P) + O_2 ($^3\Sigma_g^-$)	201.1	201.0
OBO ($^2\Pi_g$) → BOO ($^2A'$)	141.9	142.2
OBO ($^2\Pi_g$) → OBO ($^4B_1$)	101.8	101.9
B_2 ($^3\Sigma_g^-$) → 2B (^{2}P)[a]	64.3[a] [64.3]	62.8 [62.8]
BO ($^2\Sigma^+$) + B → B_2 ($^3\Sigma_g^-$) + O (^{3}P)	128.1[b] [127.9]	129.4 [129.2]
BOB ($^1\Sigma_g^+$) → B (^{2}P) + BO ($^2\Sigma^+$)	95.9	95.8
BBO ($^1\Sigma^+$) → B_2 ($^3\Sigma_g^-$) + O (^{3}P)	207.6	208.5
BBO ($^3\Sigma^-$) → B_2 ($^3\Sigma_g^-$) + O (^{3}P)	191.6	192.7
BBO ($^3\Sigma^-$) → B (^{2}P) + BO ($^2\Sigma^+$)	63.5	63.3
2BO ($^2\Sigma^+$) → B_2 ($^3\Sigma_g^-$) + O_2 ($^3\Sigma_g^-$)	202.5 [202.1]	202.5 [202.2]
OBBO ($^1\Sigma_g^+$) → 2 BO ($^2\Sigma^+$)	113.2	114.2
OBBO ($^1\Sigma_g^+$) → B_2 ($^3\Sigma_g^-$) + O_2 ($^3\Sigma_g^-$)	315.7	316.7
OBBO ($^1\Sigma_g^+$) → BBO ($^3\Sigma^-$) + O (^{3}P)	242.1	243.1
BOBO ($^1A'$) → OBO ($^2\Pi_g$) + B (^{2}P)	149.9	149.4
BOBO ($^1A'$) → BOB ($^1\Sigma_g^+$) + O (^{3}P)	180.6	181.5
BOBO ($^3A'$) → OBO ($^2\Pi_g$) + B (^{2}P)	77.1	76.7
BOBO ($^3A'$) → BOB ($^1\Sigma_g^+$) + O (^{3}P)	107.8	108.8
OBOBO ($^1A_1$) → OBO ($^2\Pi_g$) + BO ($^2\Sigma^+$)	133.8	134.9
OBOBO ($^1A_1$) → BOBO ($^1A'$) + O (^{3}P)	176.4	177.6
2OBOBO ($^1A_1$) → $2B_2$($^3\Sigma_g^-$) + $3O_2$ ($^3\Sigma_g^-$)	808.0	811.5
B_3 ($^2A_1'$) → 3B (^{2}P)	195.2	193.6
B_3 ($^2A_1'$) → B_2 ($^3\Sigma_g^-$) + B (^{2}P)	130.9	130.8
BBBO ($^4\Sigma^-$) → B_3 ($^2A_1'$) + O (^{3}P)	171.1	171.9
BBBO ($^4\Sigma^-$) → B_2 ($^3\Sigma_g^-$) + BO ($^2\Sigma^+$)	109.6	110.4
BBOB ($^4A''$) → B (^{2}P) + BOB ($^1\Sigma_g^+$)	52.0	51.8
OB_3O ($^2\Pi_u$) → BO ($^2\Sigma^+$) + BBO ($^1\Sigma^+$)	97.7	99.2
OB_3O ($^2\Pi_u$) → O (^{3}P) + BBBO ($^4\Sigma^-$)	195.8	197.3
B_4 (^1A_g) → 4B (^{2}P)	315.8	314.0
B_4 (^1A_g) → $2B_2$ ($^3\Sigma_g^-$)	187.1	188.3
B_4 (^1A_g) → B_3 ($^2A_1'$) + B (^{2}P)	120.6	120.4
2OBOBO ($^1A_1$) → B_4 (^1A_g) + $3O_2$ ($^3\Sigma_g^-$)	620.9	623.2
B_4O ($^1A_1$) → B_3 ($^2A_1'$) + BO ($^2\Sigma^+$)	99.0	99.9
B_4O ($^1A_1$) → B_4 (^1A_g) + O (^{3}P)	170.8	171.7
OBBBBO ($^3\Sigma_g^-$) → BO ($^2\Sigma^+$) + BBBO ($^4\Sigma^-$)	107.7	108.4
OBBBBO ($^3\Sigma_g^-$) → B_4O ($^3B_1$) + O (^{3}P)	205.9	206.1
OBBBBO ($^3\Sigma_g^-$) → 2BBO ($^1\Sigma^+$)	122.5	123.4
OBBBBO ($^3\Sigma_g^-$) → 2BO ($^2\Sigma^+$) + B_2 ($^3\Sigma_g^-$)	217.3	218.8

[a] Other values include: 62.5 kcal/mol (G1), refs 69 and 70; 64.1 kcal/mol (MRCI), ref 71; 69 kcal/mol (experiment), ref 72; 71.9 kcal/mol (experiment taking heats of formation of 198.3 and 135.1 kcal/mol for B_2 and B), ref 66. [b] 192.8 kcal/mol (experiment), ref 72.

TABLE 6: Adiabatic Electron Affinities of B_n and B_nO_m in eV

neutral	anion	$EA_{0K\text{-}DTQ}$ [$EA_{0K\text{-}Q5}$]	EA (exptl. or other theory)
B (^{2}P)	B^- (^{3}P)	0.26 [0.26]	0.278 ± 0.010[a]
B_2 ($^3\Sigma_g^-$)	B_2^- ($^4\Sigma_g^-$)	1.95 [1.95]	1.80[b] ≥1.30 ± 0.4[c] 3.66[d]
B_3 ($^2A_1'$)	B_3^- ($^1A_1'$)	2.88	3.20[d] 2.820 ± 0.020[e]
B_4 (^1A_g)	B_4^- ($^2B_{1u}$)	1.68	1.60 ± 0.10[f]
B_4^- ($^2B_{1u}$)	B_4^{2-} ($^1A_1$)	−2.77	
B_4 (^1A_g)	B_4^{2-} ($^1A_1$)	−1.09	
BO ($^2\Sigma^+$)	BO^- ($^1\Sigma^+$)	2.50 [2.51]	2.508 ± 0.008[g] >2.482[h] 2.832 ± 0.091[i] 2.55[j] 2.54[k]
OBO ($^2\Pi_g$)	BO_2^- ($^1\Sigma_g^+$)	4.48	4.51[l] 4.65[m]
BOB ($^1\Sigma_g^+$)	BOB^- ($^2\Sigma_g^+$)	0.07	
OBBO ($^1\Sigma_g^+$)	$OBBO^-$ (^2B_u)	0.37	
BBBO ($^4\Sigma^-$)	B_3O^- ($^3A_1$)	2.05	
OB_3O ($^2\Pi_u$)	$B_3O_2^-$ ($^3\Sigma_g^-$)	2.94	2.94 ± 0.02[n]
B_4O ($^1A_1$)	B_4O^- ($^2A_1$)	2.58	
OBBBBO ($^3\Sigma_g^-$)	$B_4O_2^-$ ($^2\Pi$)	3.14	3.160 ± 0.015[o]

[a] PES. Reference 78. [b] NIST-JANAF tables estimate. Reference 77. [c] Charge inversion mass spectrometry estimate. Reference 75. [d] Calculated at the MP4SDQ/CBSB5 level. Reference 76. [e] PES VDE. Reference 84. [f] PES ADE. Reference 84. [g] PES ADE. Reference 22. [h] Temperature-dependent equilibrium ion/molecule reaction. Reference 104. [i] Temperature-dependent equilibrium ion/molecule reaction. Reference 105. [j] Calculated at the G2 level. Reference 22. [k] Calculated at the CBS-Q level. Reference 22. [l] Ion molecule reactions. High temperature mass spectrometry. Reference 112. [m] Electron propagator theory calculations using the 6-311+G(2df) basis set. Reference 30. [n] PES VDE. Reference 23b. [o] PES VDE. Reference 23c.

only decrease the values for RE by 6 kcal/mol due to the small EA(B). This suggests that the resonance stabilization of the two compounds arises from different sources due to the different roles played by the 2s and 3s orbitals in the boron and aluminum trimers, respectively.

B4. The boron tetramer and its anion have also been the subject of a number of studies.[7,70,84,90−97] There has been a long discussion about the identity of the global minimum of the neutral cluster,[7] and the general consensus is that B_4 has a rhombic D_{2h} form with a ^1A_g ground state, due to a second-order Jahn−Teller effect.[70] The B_4 cluster has fluxional character undergoing facile structural isomerization through a square transition state (D_{4h}) with an extremely small energy barrier (<1.0 kcal/mol). The calculated B−B distance in B_4 (^1A_g) is similar to that in the trimer. In the triplet manifold, the lowest-lying state of B_4 also has the rhombic D_{2h} structure, resulting in a $^3B_{1u}$ electronic state. The B−B distance is only marginally elongated from that in the singlet. The corresponding singlet−triplet energy gap is 38.1 kcal/mol at the CCSD(T)/CBS level. The energy ordering for B_4 differs from that of Al_4, which has a $^3B_{3g}$ (D_{2h}) ground state.[40] For Al_4, the $^3B_{3u}$ and closed-shell ^1A_g states were calculated to be 2.8 and 3.3 kcal/mol above the ground state.

The TAE of B_4 has previously been calculated to be 312.2[70] and 303.0[7] kcal/mol at a modified G1 level and a CCSD(T)/6-311+G(2df) level, respectively. The G1 value is closer to our CBS value for TAE(B_4) (Table 3). Formation of B_4 from $2B_2$ is exothermic by −187.1 kcal/mol, and formation of B_4 by addition of B to B_3 is exothermic by −120.6 kcal/mol at 0 K. If we consider that there are one, three, and four B−B bonds in B_2, B_3, and B_4, respectively, the average B−B bond energies are 64.4, 65.1, and 78.9 kcal/mol, respectively. These results show that the tetramer system is stabilized with respect to B_2 or B_3.

The LUMO and LUMO+1 of neutral B_4 are not degenerate, so attachment of an electron to form the anion does not require a Jahn−Teller distortion and the anion has the neutral rhombic D_{2h} shape. Although the B−B bonds elongate only slightly to 1.583 Å in B_4^- ($^2B_{1u}$), the rhombic form is markedly distorted upon electron attachment in such a way that the diagonal distance is changed from 1.933 Å in the singlet neutral to 1.659 Å in the doublet anion. Our results concur with recent theoretical results that the ground electronic state of B_4^- is the $^2B_{1u}$ state[7,96] rather than the ^2A_g state.[95] We found the lowest-lying high spin $^4B_{1u}$ state to be 26.0 kcal/mol higher than the ground $^2B_{1u}$ state. Our CCSD(T)/CBS adiabatic electron affinity of the boron tetramer is 1.68 eV. The VDE(B_4^-) was calculated to be 0.13 eV smaller than the experimental VDE,[84] a larger difference

TABLE 7: Vertical Attachment Energies (VAE) and Vertical Detachment Energies (VDE) for B_nO_m Structures in eV at the CCSD(T)/aVQZ Level

	VAE		VDE [VDE_{expt}]
B_2 ($^3\Sigma_g^-$) + 1e → B_2^-	1.92	B_2^- ($^4\Sigma_g^-$) → B_2 + 1e	1.95
B_3 ($^2A_1'$) + 1e → B_3^-	2.85	B_3^- ($^1A_1'$) → B_3 + 1e	2.85 [2.82 ± 0.02][a]
B_4 (^1A_g) + 1e → B_4^-	1.67	B_4^- ($^2B_{1u}$) → B_4 + 1e	1.86 [1.99 ± 0.05][a]
BO ($^2\Sigma^+$) + 1e → BO^-	2.46	BO^- ($^1\Sigma^+$) → BO + 1e	2.56
OBO ($^2\Pi_g$) + 1e → BO_2^-	4.53	BO_2^- ($^1\Sigma_g^+$) → OBO + 1e	4.53
BOB ($^1A_1$) + 1e → BOB^-	−0.001	BOB^- ($^2\Sigma_g^+$) → BOB + 1e	0.03
OBBO ($^1\Sigma_g^+$) + 1e → $OBBO^-$	0.15	$OBBO^-$ (^2B_u) → OBBO + 1e	0.74
BBBO ($^4\Sigma^-$) + 1e → B_3O^-	1.89	B_3O^- ($^3A_1$) → BBBO ($^4\Sigma^-$) + 1e	2.22
OB_3O ($^2\Pi_u$) + 1e → $B_3O_2^-$	2.90	$B_3O_2^-$ ($^3\Sigma_g^-$) → OB_3O + 1e	3.00 [2.94 ± 0.02][b]
B_4O ($^1A_1$) + 1e → B_4O^-	2.65	B_4O^- ($^2A_1$) → B_4O + 1e	2.67
OBBBBO ($^3\Sigma_g^-$) + 1e → $B_4O_2^-$	3.08	$B_4O_2^-$ ($^2\Pi$) → OBBBBO + 1e	3.16 [3.16 ± 0.015][c]

[a] Referenc 84. [b] Reference 23b. [c] Reference 23c.

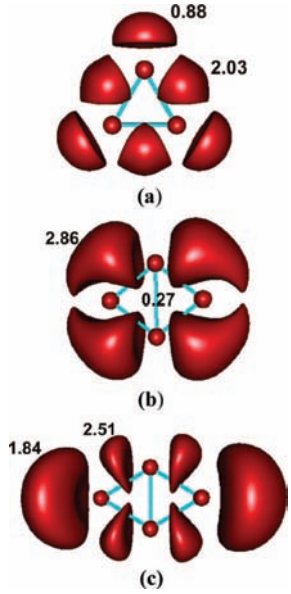

Figure 1. ELF isosurfaces of boron clusters (a) B_3, (b) B_4, and (c) B_4^{2-}. The isosurfaces are in the range of 0.76−0.86. Wave functions were generated by using the B3LYP/aug-cc-pVDZ calculations. Red ball is oxygen, and blue ball is boron. Electronic populations (in electrons) are given on valence basins.

than expected. There is a difference of ~0.2 eV between VAE and VDE (Table 7) as well as between the EA and the VDE. The calculated EA is in agreement with the experimental EA considering the experimental error bars.

The adiabatic EAs of boron clusters increase from 0.26 eV for B to 1.95 eV for B_2, to 2.88 eV for B_3 and decrease to 1.68 eV for B_4. The tetramer EA is reasonably large for a closed-shell molecule. This sequence differs from that previously determined for the heavier aluminum clusters, where the EAs increase from Al (0.41 eV) to Al_2 (1.51 eV) to Al_3 (1.89 eV) to Al_4 (2.18 eV).[40] The decrease in the EA from B_3 to B_4 can be explained on the basis of the radical nature of the trimer. The B_3^- anion has strong aromaticity with its 10 valence electrons.[7] The more voluminous Al_4 is better able to attach the excess electron than B_4. With a $^2B_{1u}$ ground state, the B_4^- anion is as a π-type radical and differs from the heavier Al_4^- congener. The Al_4^- anion has a rhombic form but a ^2A_g ground state resulting from the partial occupation of the σ in-plane symmetric a_g orbital. In addition, the two other lower-lying doublet states $^2B_{2\,g}$ and $^2A_{2u}$ of Al_4^- are nearly degenerate and only ~3 kcal/mol above the ground state.[40] The intrinsic difference in the electronic structure of the elements B and Al, and that between B_4 and Al_4 in their way of reorganizing the electron distribution upon electron attachment leads to the difference in the EA's ordering stated above.

The differences between B and Al clusters are clearly shown in the corresponding dianions B_4^{2-} and Al_4^{2-}, which have each a closed-shell electronic structure and 14 valence electrons. The planar square-shaped structure of the aluminum tetramer dianion has been shown to be a prototypical all-metal species having a 3-fold (σ, σ, and π) aromaticity.[40] Sundolm and co-workers[98] considered for B_4^{2-} only a square D_{4h} structure and investigated its molecular structure and magnetic properties up to the CCSD(T)/TZV2P level. We confirm that the D_{4h} ring is a local energy minimum of B_4^{2-} ($^1A_{1g}$), but we found that a rhombic D_{2h} structure (^1A_g) is 8.5 kcal/mol lower in energy than the D_{4h} ring. The B−B distance calculated for the D_{4h} ring is larger than that of the D_{2h} ring. The former value is comparable to that of 1.647 Å reported previously.[98] With a heat of formation of 254.0 kcal/mol at 0 K, the B_4^{2-} dianion is not stable with respect to electron detachment to form either B_4 (229.0 kcal/mol) or B_4^- (190.2 kcal/mol). In contrast, the Al_4^{2-} dianion lies ~18 kcal/mol below the neutral Al_4 but is ~35 kcal/mol above the anion Al_4^-.[40] Again, the Al tetramer has a larger propensity to capture electrons. We note that the instability of B_4^{2-} to electron detachment may raise issues[99,100] with the actual values for the energetic, but we present these values as an aid in understanding these species.

The orbitals for B_4^{2-} are clearly different from those in Al_4^{2-} (Figure 2b). The NHOMO for Al_4^{2-} and B_4^{2-} are the same, and the HOMO−2 in Al_4^{2-} is the same as HOMO−3 in B_4^{2-}. However, the remaining σ orbitals in the boron cluster are quite different from those in the aluminum cluster.

Following our work on the Al_4^{2-} anion,[40] the RE of B_4^{2-} is defined by eq 5:

$$RE(B_4^{2-}) = \Delta E(B_4^{2-} \rightarrow 4B + 2e) - m\Delta E(B_2(^3\Sigma_g) \rightarrow 2B) \quad (5)$$

For Al_4^{2-}, the 3s orbitals are substantially separated from the 3p orbitals, so we used $m = 3$ because each Al atom contributes one bonding 3p electron to the dianion, and thus Al_4^{2-} has a total of six bonding electrons leading to $m(Al_4^{2-}) = 3$. In B_4^{2-} using 6 active electrons as in Al_4^{2-}, we obtain $RE(B_4^{2-}) = 98$ kcal/mol as compared to $RE(Al_4^{2-}) \approx 73$ kcal/mol. The RE in B_4^{2-} is much less than that in B_3^- at the comparable level. If we assume in our model for RE that $m = 4$, $RE(B_4^{2-}) = 33$ kcal/mol, considerably less than in B_3^- or Al_4^{2-}. The resonance energy in the latter model for B_4^{2-} is comparable to that of benzene.[101] A better estimate of the resonance stabilization

energy in these systems may be to look at the B_4^- ion, which is stable to electron detachment. Using eq 6,

$$RE(B_4^-) \approx \Delta E(B_4^- \rightarrow 4B + 1e) - m\Delta E(B_2(^3\Sigma_g) \rightarrow 2B) \quad (6)$$

with $m = 4$, we obtain $RE(B_4^-) = 97$ kcal/mol, suggesting substantial stabilization in B_4^-. We can estimate $RE(Al_4^-)$ to be 108 kcal/mol by using the same expression previously employed[40] for $RE(Al_4^{2-})$ as shown in eq 7 and the previously obtained atomization energies.

$$RE(B_4^-) \approx \Delta E(Al_4^- \rightarrow 4Al + 1e) - 3\Delta E(Al_2(^1\Sigma_g) \rightarrow 2Al) \quad (7)$$

Thus, the REs for Al_4^- and B_4^- are quite similar as found for Al_3^- and B_4^- when similar expressions were used. Overall, the closed-shell four-member dianion B_4^{2-} is an aromatic system despite its instability with respect to electron detachment, suggesting that it might be possible that B_4^{2-} could be trapped as a ligand in various coordination complexes.

In the ELF of B_4 (Figure 1b), most of the electrons are located in the four (BB) basins, with ~2.9 electrons each, and a small but non-negligible amount (0.3 electron) is concentrated at the center of the ring, suggesting a weak bonding interaction between the close pair of diagonal boron atoms. In the rhombic dianion shown in Figure 1c, each of the four (BB) basins contains ~2.5 electrons and each of the two nonbonding basins ~1.8 electrons. A small amount of electron density exists on the short B−B diagonal as in the neutral cluster. Although both B_4 and Al_4 have rhombic shapes, the mixed B_3Al and BAl_3 species prefer triangular structures with B_3Al formed from addition of Al to the B_3 cycle,[102] and BAl_3 adopting a structure in which B occupies a central position.[103]

Boron Oxides (B_nO_m) and Their Anions. Figures 3, 5, 6, and 7 show the (U)CCSD(T)/aVTZ optimized geometries of the neutral oxides and their anions. Figures 3 and SM-1 (Supporting Information) display the ELF pictures of various oxides in their ground state. Tables 1 and 2 give a comparison of calculated results with available experimental data for bond distances and vibrational frequencies.

BO. The boron monoxide radical has been studied by a variety of spectroscopic techniques.[12,13,16,17,21,22,72] We considered both the ground $X^2\Sigma^+$ state and the excited $A^2\Pi$ state. The calculated distances of the two states are 0.01 Å larger than the corresponding experimental values.[72] The R/UCCSD(T)/aVQZ harmonic stretching frequencies are slightly smaller than the experimental values,[16b] consistent with the longer bond lengths; the calculated value of $\omega_e\chi_e$ is in excellent agreement with experiment. The excitation energy for the $A^2\Pi \leftarrow X^2\Sigma^+$ electronic transition is calculated as $T_e = 2.94$ eV (67.8 kcal/mol at 0 K), in excellent agreement with the experimental result of 2.96 eV.[72] Previous CISD-Q calculations led to a smaller value of 2.72 eV.[34] The calculated bond dissociation energy BDE(BO) is in excellent agreement with the experimental value.[72] Although the diatomic B−O bond is very strong, analysis of the electron density does not show a particular electron concentration between both atoms. The ELF plots (Figure 4) show that there is one disynaptic basin V(B,O) containing only ~3.0 electrons, a nonbonding basin (V(B) = 1.2 electrons) corresponding to the unpaired electron on B, and a large nonbonding V(O) basin of 4.6 electrons of the O lone pairs, in line with the high polarity of the diatomic molecule (dipole moment of 2.9 D at the HF/aVTZ level).

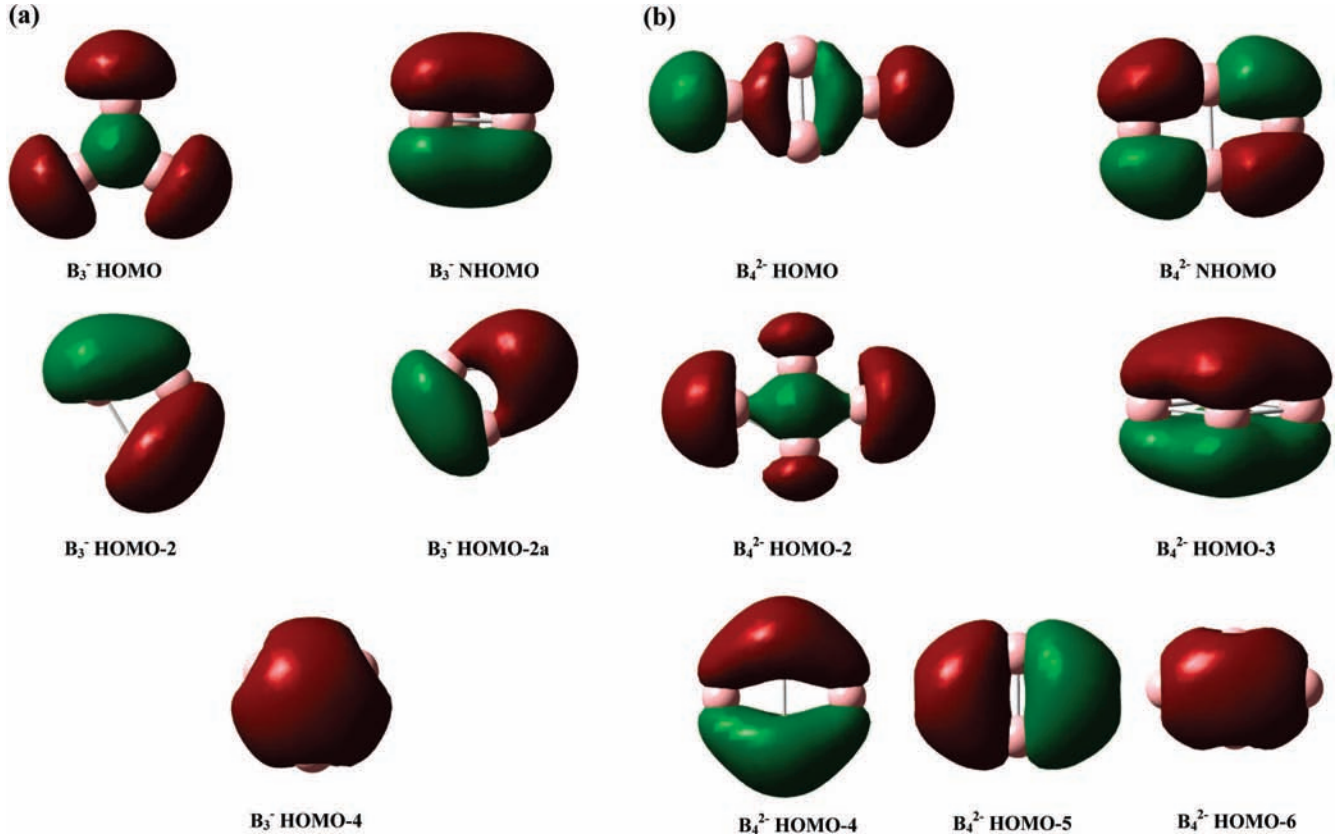

Figure 2. Valence occupied orbitals for (a) B_3^- and (b) B_4^{2-}.

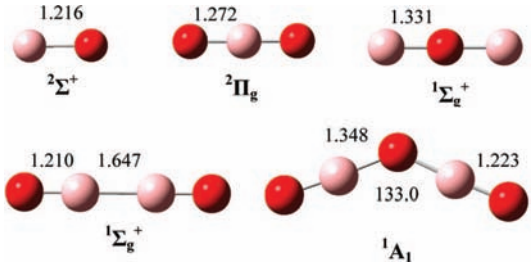

Figure 3. (U)CCSD(T)/aVTZ optimized geometries of neutral B_nO_m ($n = 1-2$, $m = 1-3$), together with the symmetry of the ground electronic states. Bond lengths are given in angstroms, and bond angles are in degrees.

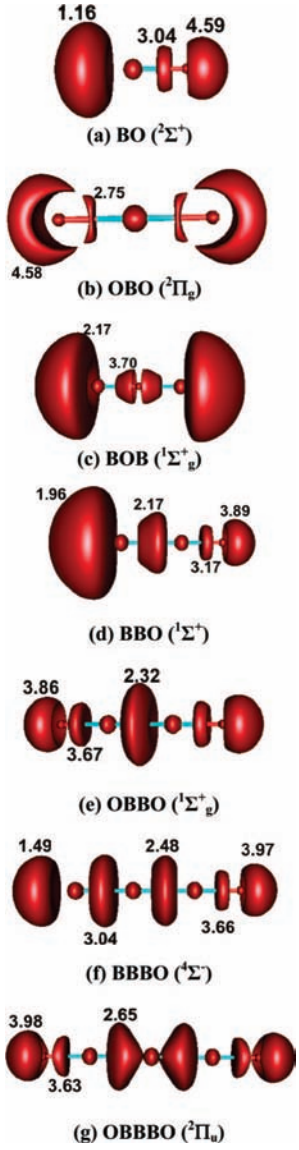

Figure 4. ELF isosurfaces of boron oxides having one, two, and three boron atoms. Isosurfaces are in the range of 0.76−0.86. Wave functions were generated by using the B3LYP/aug-cc-pVDZ calculations. Red ball is oxygen, and blue ball is boron. Electronic populations (in electrons) are given on valence basins.

The BO^- anion has a closed-shell $^1\Sigma^+$ state, similar to the isoelectronic cyanide CN^- anion. According to the population analysis, there is a lone pair B, but the negative net charge is still located on the oxygen.[31] The calculated BO distance and harmonic stretch frequency in good agreement with the photoelectron spectroscopy (PES) result considering the experimental error bars.[22] The calculated EA(BO) is in excellent agreement with the PES value and an earlier result of >2.482 eV[104] but not with another earlier value.[105] The latter two approaches measured the temperature-dependent equilibria of ion/molecule reactions. The G2 and CBS-Q calculated EAs are in reasonable agreement with our result.[22] For this diatomic species, both VAE and VDE are about the same as the adiabatic EA (Table 7).

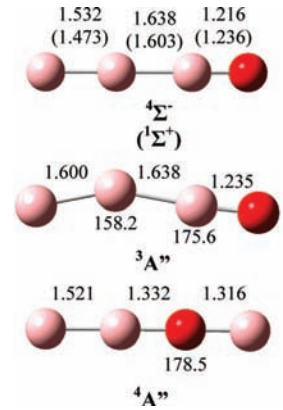

Figure 5. (U)CCSD(T)/aVTZ optimized geometries of different isomers for B_3O neutral and B_3O^- anion (given in parentheses), along with their electronic state. Bond lengths are given in angstroms, and bond angles are in degrees.

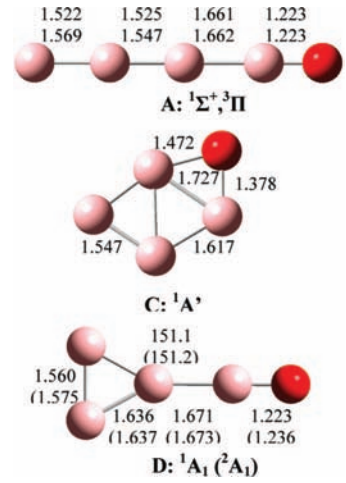

Figure 6. (U)CCSD(T)/aVTZ optimized geometries of B_4O neutral and anionic isomers (given in parentheses), with their electronic state. See text for definition of forms **A**, **C**, and **D**. Bond lengths are given in angstroms, and bond angles are in degrees.

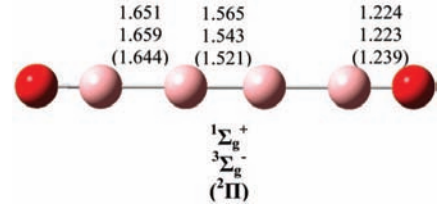

Figure 7. (U)CCSD(T)/aVDZ optimized geometries of the linear structure of neutral B_4O_2 and anionic $B_4O_2^-$ (given in parentheses). Bond lengths are given in angstroms, and bond angles are in degrees.

BO_2. The $X^2\Pi_g-A^2\Pi_u$ transition of the boron dioxide has been the subject of several experimental studies using electronic[18−20] and vibrational[13,14] spectroscopies. We considered both OBO and BOO isomers in the lowest-lying doublet state. The quartet states for both structures are of higher energy. OBO is

linear, and the calculated B−O bond distance is in good agreement with the experimental values.[106,107] The BOO isomer is bent in its $^2A'$ ground state with comparable BO and OO distances of ∼1.35 Å. It has been established that MO methods have encountered difficulties in reproducing the vibrational fundamentals of OBO.[30] The main issue is with the asymmetric stretch.[13,19,20,25,108,109] In the ground $^2\Pi_g$ state of OBO, the experimental asymmetric stretch of 1278 cm^{-1} is larger than the symmetric stretch of 1056 cm^{-1}. Calculations predict the opposite order with the symmetric stretch of 1095 cm^{-1} slightly larger than the asymmetric stretch of 1055 cm^{-1} (cf., Table 2). The value for the symmetric mode is predicted reasonably well, but the asymmetric mode is predicted to be ∼220 cm^1 too low. Because of this difference, we used the experimental values in the prediction of the ZPE. An ELF analysis indicates that the two V(B,O) basins have each a population of 2.7 electrons, and the total population around B is up to 5.5 electrons, corresponding to a radical center at the central boron atom (Figure 4).

The lowest $^4B_1$ structure of OBO is nearly cyclic, and the doublet−quartet gap is 4.40 eV (101.5 kcal/mol, Table 4). The linear ground-state doublet of OBO is 141.5 kcal/mol more stable than the bent BOO isomer. The calculated heat of formation at 298 K for OBO is lower than and just outside the JANAF experimental error limits ± 2.0 kcal/mol.[61] It differs even more from the value obtained from mass spectrometry experiments on OBO^-.[110] The T_1 diagnostic for ground-state OBO is 0.016, suggesting that the single-reference approach is valid for this radical. This difference coupled with the difficulty in calculating the asymmetric stretch suggests that higher order excitations on the order of 2−3 kcal/mol could be important. The average BO bond energy is 159.4 kcal/mol, smaller than the value in BO, and the initial BO bond breaking of OBO → O + BO is less endothermic than breaking the second bond.

The BO_2^- anion was generated and characterized by IR spectroscopy in an Ar matrix.[13] Vibrational data are consistent with a linear OBO^- anion with a closed-shell $^1\Sigma_g^+$ ground state isoelectronic to CO_2. On electron attachment, the BO distance remains almost unchanged (1.272 Å), but the asymmetric stretch frequency is significantly blue-shifted. The calculated harmonic frequencies are in good agreement with the observed values for the asymmetric stretch and the bend from solid Ar IR experiments (cf., also Table 2).[13] The vibrations of OBO^- are also consistent with numerous results obtained for MBO_2 salts involving metals (M = Li, Cs).[111] The difference between the VDE or ADE and the adiabatic EA is only 0.1 eV. Earlier electron propagator theory calculations using the 6-311+G(2df) basis set led to a comparable value for the EA.[30] The experimental results are rather disparate ranging from 3.28 to 4.51 eV.[77] The most recent value of 4.32 ± 0.21 eV[110] is from mass spectrometry experiments. Our ADE, 4.48 eV, is consistent with the higher range of experimental values.[77,112] Both VAE and VDE values are again similar to each other and to the adiabatic value. The ability of the triatomic BO_2 to capture an electron is markedly enhanced as compared to diatomic BO.

B_2O. We considered the BBO and BOB isomers in both the singlet and the triplet manifolds. Our calculations concur with previous findings[28,39] that the linear $^1\Sigma^+_g$ BOB is the most stable isomer with the linear $^1\Sigma^+$ BBO 16.7 kcal/mol higher at 298 K. The equilibrium structure (r_e) of singlet BOB deviates slightly from linearity with a BOB angle of 166.0°, but bending leads to an energy gain of <0.01 kcal/mol. With a ZPE correction of 0.09 kcal/mol, the r_o structure would be linear. Thus, BOB is a centro-symmetric linear structure with fluxional character.

A reverse ordering of the energies is predicted for the triplet manifold. BOB has two distinct structures with the bent (nearly cyclic) $^3B_2$ state 26.9 kcal/mol below the linear $^3\Pi_u$ form. BBO ($^3\Pi$) is 7.0 kcal/mol lower in energy than BOB ($^3B_2$). The singlet−triplet gaps are 16.0 and 39.4 kcal/mol for BBO and BOB, respectively, and the lowest triplet isomer BBO is 32.3 kcal/mol above the ground-state singlet BOB. For TAE(BOB,$^1\Sigma^+_g$), previous theoretical results of 289.5 (G1 level) and 288.7 (modified G1 method) kcal/mol[28] compare well with our CCSD(T)/CBS value. The present CBS heat of formation of BOB is within the ±25 kcal/mol error limits of the estimated JANAF values.[61] The average BO bond energy of 144.1 kcal/mol in singlet BOB is smaller than those of BO and OBO.

The ELF populations are shown in Figure 4 for both singlet BOB and BBO structures. The V(B,O) basin in BOB (3.7 electrons) contains more electrons than that of BBO (3.2 electrons). Each terminal B atom possesses a lone pair of ∼2 electrons. The B−B bond in BBO has single bond character, consistent with the long B−B distance and the B−B harmonic frequency of 631 cm^{-1}. As compared to the values for $^3B_2$ (ω = 1039 cm^{-1}), the calculated parameters of BBO suggest a weakening of the BB bond and a strengthening of the BO moiety following the binding of O(^{3}P) to $B_2(^3\Sigma_g^-)$. The oxidation of B_2 by O is highly exothermic (−207.6 kcal/mol). The addition of B(^{2}P) to BO($^2\Sigma^+$) producing singlet BOB is less exothermic (−95.9 kcal/mol).

The $^2\Sigma_g^+$ state is found to be the ground state for the BOB^- anion, and this state is 49 kcal/mol lower than the $^4\Sigma_g^-$ state. The electron in the anion is only bound by 1.7 kcal/mol. The vertical VAE and VDE values are very small (Table 7).

B_2O_2. This tetraatomic species was generated in the gas phase more than half-century ago when a mixture of boron and B_2O_3 solids was heated to ∼1200 °C.[113] A centro-symmetric structure OBBO was initially assumed, but a bent OBOB structure was subsequently proposed as an alternative.[114] Early semiempirical (MNDO) and ab initio HF/STO-3G calculations showed the linear OBBO to be more stable.[115] Later, the species was produced in Ar matrix experiments and identified by IR spectroscopy.[13] Its photoelectron spectrum was also measured.[21] The linear OBBO is consistent with spectroscopic data, as well as found by more recent DFT-MD simulations.[39] Experiments have suggested the production of OBBO in a B_2-O_2 mixture under ultraviolet photolysis.[116]

We considered both OBBO and OBOB isomers in the lowest singlet and triplet states. Whereas OBBO is linear in both the singlet and the triplet states, OBOB is bent. OBBO ($^1\Sigma_g^+$) is the most stable structure with OBOB ($^1A'$) 29.1 kcal/mol higher in energy. Both triplet states are much higher in energy, with singlet−triplet gaps of 78.2 (for OBBO) and 72.8 (for OBOB) kcal/mol (Table 4). The long B−B bond distance in OBBO ($^1\Sigma_g^+$) is consistent with an ELF population of ∼2.3 electrons for the V(B,B) basin as illustrated in Figure 4. The vibrational spectra of OBBO have been analyzed in detail in previous studies[13,21,39,117] (cf., Table 2), and our calculated results are in excellent agreement with the available experimental values.[13]

The CCSD(T)/CBS heat of formation at 298 K is in excellent agreement with the value obtained from equilibrium vapor pressure methods.[61] The combination of two BO radicals to form OBBO does not induce a significant change in the BO bond, and the new B−B bond is ∼0.05 Å longer than that of diatomic B_2. Despite this increase in the bond length, the B−B bond in OBBO is nearly twice as strong as that in B_2. Formation of OBBO from the dimerization of BO is exothermic by −114.2 kcal/mol (at 298 K) as compared to a diatomic B−B bond

strength of 64.3 kcal/mol. The B−O BDE (OBBO → ^{3}O to ^{3}BBO) is 242.6 kcal/mol. The oxidation of B_2 by O_2 releases 316.7 kcal/mol. The higher energy bent OBOB form has a nearly linear OBO framework bonded to the second B atom The B−OBO BDE is 180.6 kcal/mol. In the triplet state, it is relatively easier to break the OBOB bonds (Table 5).

Electron addition to the OBBO skeleton leads to a trans-bent configuration (C_{2h}) for the $B_2O_2^-$ anion with a low spin ^2B_u ground state. The adiabatic EA is relatively small, 0.37 eV. Because of the large geometrical distortion, there are noticeable differences in the VAE and VDE (Table 7).

B_2O_3. Diboron trioxide is a stable solid, which plays an important role in modern ceramic and glass technology.[118] In the gas phase, its molecular structure was controversial for a long period spanning the 1960s and 1970s.[119] The critical point was whether the molecule (OBOBO) is bent or linear. It has been established that B_2O_3 has a V-shaped C_{2v} structure, similar to the isoelectronic dicyanoether.[120] The calculated BO terminal and central distances are of the same order of magnitude as those in various species discussed above and are in fairly good agreement with the experimental values.[107] The central OBO bond angle is large, and the molecule only deviates marginally from linearity. Our calculations confirm the fluxional character of B_2O_3, which bends extremely easily at the central oxygen, with an energy barrier from bent to linear <0.5 kcal/mol,[120,121] so B_2O_3 can be regarded as a quasi-linear structure. The CCSD(T)/aVDZ terminal B−O harmonic frequencies split by only 3 cm^{-1} and are slightly smaller than the experimental value recorded for the most naturally abundant $^{11}B^{16}O$ isotopomer. The CCSD(T)/CBS for the heat of formation of OBOBO at 298 K differs by 1.5 kcal/mol from the experimental value obtained from heats of vaporization, which has an error bar of ±1.0 kcal/mol.[61] In the gas phase, breaking the central BO bond (B_2O_3 → BO + OBO) requires 135.2 kcal/mol, and, as expected, cleavage of a terminal BO (OBOBO → O + BOBO) requires more energy, 177.1 kcal/mol. The closed shell singlet molecule does not bind an electron.

B_3O. In the previous DFT-MD study,[39] a linear BBBO quartet ground state was reported as the most stable isomer. This tetraatomic radical can be considered as forming from either B_3 + O or a B_2 + BO recombination reaction. Figure 5 gives a summary of the B_3O structures. We could not locate a local minimum in which O binds with either one or two B atoms of a B_3 triangle in both doublet and quartet states. In the quartet state, we found two equilibrium chain structures with a linear BBBO ($^4\Sigma^-$) and a marginally bent BBOB ($^4A''$). BBBO ($^4\Sigma^-$) is 26.0 kcal/mol more stable than BBOB ($^4A''$). In the doublet manifold, a chain BBBO structure does not correspond to a local minimum, whereas a BBOB form having a marginally bent BOB moiety ($^2A'$) is a local minimum and is 27.3 kcal/mol above the related $^4A''$ structure. We show the energetic results for the two lowest-lying $^4\Sigma^-$ and $^4A''$ isomers in Tables 3 and 4. Thus, in agreement with previous findings, high spin linear BBBO ($^4\Sigma^+$) is the most preferred form for B_3O. The B−B bond dissociation energy of BBBO giving B_2 + BO is 110.4 kcal/mol, and the B−O BDE (B_3 + O) is 171.3 kcal/mol. The B−B BDE in BBOB (B + BOB) is much smaller, 52.0 kcal/mol.

The electronic distribution of BBBO (Figure 4) suggests a Lewis dot structure of ·B═B−B═Ö:. Because of electron delocalization, the valence basin of the central bond V(B,B) has ∼2.5 electron. The stable quartet structures can be considered as being formed by a linear approach of the triplet B_2 to either end of the doublet BO, without changing the spin state, which results in high spin adducts. Energetically, B−B bonding giving BBBO is favored over B−O bonding giving BBOB.

The equilibrium structure of the triplet $BBBO^-$ isomer is calculated to be linear ($^3\Sigma^-$) at the MP2 level, but bent ($^3A''$) at the CCSD(T) level (Figure 5). The energy difference between the bent and linear forms is very small (<0.5 kcal/mol), and the anion can be considered as a quasi-linear structure. In the singlet state, the $BBBO^-$ anion is linear at all levels considered. The $^3A''$ state is lower than the $^1\Sigma^+$ state by 34.0 kcal/mol. The $BBOB^-$ anion isomer has a low spin state ($^1\Sigma^+$), but it is not bound with respect to electron detachment. The adiabatic electron affinity of B_3O is smaller than the values of either B_3 or BO and slightly larger than that of B_2. Considering BBBO as a substituted B_2, the EA of B_2 is enhanced by the BO substituent. As expected, the bending in the $BBBO^-$ anion gives rise to a difference (0. 33 eV) between the VAE and VDE.

B_3O_2. A linear doublet OBBBO structure was predicted as the most stable isomer for this pentaatomic cluster.[39] Wang and co-workers[23] produced the $B_3O_2^-$ anion in the gas phase and characterized its energetics by PES. We considered various structures arising from interactions of B_3 with O_2 and B_3O with O. Adducts from (B_3 + O_2) are too high in energy and will not be further discussed (cf., Table 3 for the $^2A_1$ and $^2B_1$ states of B_3O_2). Binding a triplet O atom at the B end of the linear quartet BBBO leads to OBBBO products having a variety of possible structures and spin states. Our calculations concur with previous DFT-MD results[39] that for the centro-symmetric OBBBO radical, the low spin $^2\Pi_u$ state is the ground state, 98.8 kcal/mol lower in energy than the high spin $^4\Pi_u$ state. The ELF plots (Figure 4) suggest that insertion of a B atom between two BO groups leads to a Lewis structure of the type: Ö═B−B·−B═Ö: in which the unpaired electron is concentrated on the middle B center, resulting in a doublet state. This is consistent with the calculated BB and BO bond distances of 1.618 and 1.218 Å, respectively.

The PES spectrum of the anion shows a vibrational frequency of 1950 ± 40 cm^{-1} for the neutral species.[23] The two components of the UMP2/aVTZ harmonic BO stretch frequencies are split by ∼20 cm^{-1} and are in excellent agreement with the PES result. These stretches are increased relative to the corresponding mode in the BO radical of ∼1900 cm^{-1}. The B−B BDE (BBO + BO) is 99.2 kcal/mol.

The $OBBBO^-$ anion can be either a singlet or a triplet. The linear $^3\Sigma_g^-$ state is confirmed to be the ground state.[23] Upon electron attachment, both BO and BB distances are only marginally changed in the triplet anion as compared to the neutral. The increase of the anion BO distances is consistent with a red shift of their stretch frequencies to 1834 (σ_g) and 1830 cm^{-1} (σ_u) (MP2/aVTZ). The two unpaired electrons are localized on the central B atom. Considering OBBBO as a derivative of BH_2 ($B(BO)_2$), then its anion is a derivative of BH_2^-, which is isoelectronic with methylene. CH_2 has a triplet ground state, and the singlet−triplet splitting is very small for BH_2^- (see Supporting Information).[122] The BO substituent does not change the multiplicity and can be considered as an electropositive species. Relative to the triplet ground state, the closed-shell linear $^1\Sigma_g^+$ state has a nearly identical geometry and slightly smaller BO stretch frequencies of 1805 (σ_g) and 1804 cm^{-1} (σ_u). The singlet−triplet gap in $B(BO)_2^-$ is at 15.0 kcal/mol at 0 K, which can be compared to values of 9.2 kcal/mol for CH_2 (experimental value[123] of 9.0 ± 0.09 kcal/mol) and 0.0 ± 0.2 kcal/mol for BH_2^-, obtained as described below. BH_2^- is predicted to have a ground-state triplet at the bottom of the potential well with the singlet 0.44 kcal/mol higher in

energy (see Supporting Information). This is smaller than the value of 1.02 kcal/mol previously reported at the multireference configuration interaction (MRD-CI) level with a polarized triple-ζ basis set with some diffuse functions.[122] The ZPE is larger in the triplet than in the singlet by 0.58 in our approach, and the same value is found in a more detailed study of the vibrations.[122] Thus, we would predict that the singlet becomes the ground state when ZPE is included by 0.1 kcal/mol. We found an error of approximately 0.2 kcal/mol for the singlet−triplet splitting in CH_2 at the same level, so our best estimate for the singlet−triplet splitting in BH_2^- is 0.0 ± 0.2 kcal/mol. Thus, each BO substituent in $B(BO)_2^-$ stabilizes the triplet by 7.5 kcal/mol.

The calculated adiabatic EA of B_3O_2 ($^2\Pi_u$) is in excellent agreement with the PES value.[23a] Previous B3LYP/aVTZ calculations predicted a slightly higher value of 3.01 eV for this quantity.[23a] Contrary to experiment, we found a small difference of 0.1 eV between the vertical ADE and VDE.

B_4O. The structural features of the tetraboron monoxide system are summarized in Figure 6. Drummond et al.[39] reported three different types of structure, including a linear form **A** (BBBBO), a planar cyclic form **B** in which the O atom binds to one B center of the B_4 ring along the diagonal BB axis (C_{2v}), and a planar cyclic form **C** in which O bonds with two B atoms of the B_4 ring forming a bridge (C_s). All of the reported structures were for the triplet state. We considered here not only the closed-shell singlet state, but also another possible isomer **D** in which a BO radical simply binds at its B end to one B atom of a B_3 ring, forming an exocyclic linear BBO frame along the C_2 axis (being perpendicular to the remaining ring BB bond).

In the linear framework **A**, the $^3\Pi$ state is 29.0 kcal/mol more stable than the $^1\Sigma^+$ state. Isomer **B** is not confirmed to be an energy minimum. Geometrical relaxation invariably gives rise to the bridged isomer **C** (Figure 6). In the C_s isomer **C**, the $^1A'$ state is 36.9 kcal/mol more stable than the $^3A'$ state. The singlet has not been previously reported. For isomer **D**, the $^1A_1$ state is a local minimum, and no local minimum could be found for the $^3B_1$ state. The **D**($^1A_1$) state is the global minimum for the structures that we studied with the **C**($^1A'$) state about 1 kcal/mol higher in energy. Both the **D**($^1A_1$) and the **C**($^1A'$) states are ∼35 kcal/mol more stable than the linear **A**($^3\Pi$) state. The high energy character of **A** can be accounted for by the fact that neither the B_3 nor the B_4 clusters exist in this form. The higher stability of **C** and **D** can be explained by considering the involvement of the B_4 and B_3 rings, respectively. Binding of either O to B_4 giving **C** or BO to B_3 yielding **D** is exothermic by 171.2 (**C**) and 99.3 (**D**) kcal/mol, respectively (values at 298 K, Table 5). The latter is less stable with respect to bond cleavage because both products are relatively stable, and each has an unpaired electron on a B atom. The ELF plots (Figure SM-1) show that isomer **C** has two BO bonds with a bridging O atom and a total electronic population of ∼3 electrons, which is much smaller than that of the nonbonding basin of oxygen V(O). Isomer **D**, composed of a B_3 cluster with a BO bonded to it, has a single BB bond (Figure SM-1). The terminal BO bond of **D** has a typical distance of ∼1.23 Å and stretching frequency of 1946 cm^{-1}.

Electron attachment to **D** does not modify the molecular shape (C_{2v}) in forming the anion $^2A_1$ ground state (Figure 6). Although the neutral **D** isomer is a closed-shell species, its adiabatic EA of 2.58 eV is considerable and of the same order of magnitude as those of the components BO (2.50 eV) and B_3 (2.80 eV). In contrast to B_3O, if B_4O is considered as a BO-substituted B_3, its EA is slightly reduced relative to that of B_3. Further work is required to understand the role of the B═O substituent on electron affinities in boron oxide clusters.

B_4O_2. The tetraboron dioxide system has been described in detail in two recent studies. As for B_3O_2, Drummond et al.[39] studied this molecule using DFT-MD methods. Wang and coworkers[23b] carried out both experiments and calculations (DFT using B3LYP and B3PW91 functionals, as well as MP2, CCSD(T), and CASPT2) for this boron oxide. The latter authors characterized the gaseous phase $B_4O_2^-$ anion and $B_4O_2^{2-}$ dianion using a combination of MS/PES techniques and determined the ADE and VDE of the system.

We located different isomers in different spin states and confirm that the B_4O_2 cluster is a linear OBBBBO chain with a $^3\Sigma_g^-$ ground state. The corresponding $^1\Sigma_g^+$ state is also a local minimum, with a singlet−triplet gap of 14.6 kcal/mol. The calculated bond distances in both linear states are quite close to each other (Figure 7) and do not show any particular deviation from the values predicted for the smaller clusters discussed above. Similarly, the harmonic frequencies of 1940 (σ_g) and 1928 cm^{-1} (σ_u) for the triplet are those expected for BO stretch frequencies. The most striking feature of B_4O_2 is that it does not involve either a B_3 or a B_4 ring in its most stable isomer. Isomers containing these rings are calculated to be from 35 to 100 kcal/mol (or even more) higher in energy.

The ELF plots (Figure SM-1) show that, although a high degree of electron delocalization is present in the neutral molecule, it is mainly composed of two B═O bonds and three B−B bonds, yielding a Lewis structure of the type: Ö═B−B•−•B−B═Ö:. The unpaired α electrons are localized mostly on the two central boron atoms (1.3 electrons each). The linear triplet isomer arises from bonding two BO radicals at their B ends to the each end of a triplet B_2. This condensation reaction is exothermic by −218.8 kcal/mol (at 298 K). As in B_3O, the B_4O_2 adduct has strong BO bonds, 205.6 kcal/mol (OBBBBO → ^{3}OBBBB + ^{3}O). The strong B═O bonds leads to the linear adduct being favored over the cyclic isomers containing either a triangular B_3 or a rhombic B_4 unit, which would break these strong bonds. Homolytic dissociation of the B−B(O) bond (BO + BBBO($^4\Sigma^-$)) requires 108.4 kcal/mol, and of the central B−B bond (2 BBO ($^1\Sigma^+$)) requires 123.4 kcal/mol. These can be compared to C−C σ bond energies of 90 kcal/mol in C_2H_6 at 298 K and 109 kcal/mol in C_2H_4.[41d,124]

The $B_4O_2^-$ anion maintains the linear skeleton in its $^2\Pi_u$ ground state, which is ∼43 kcal/mol lower than the $^3\Pi_u$ state. The presence of the additional electron leads to a decrease in all three BB bonds of up to 0.04 Å and a small increase in the terminal BO bonds (Figure 7). The unpaired electron still resides on the central BB moiety. The adiabatic electron affinity of B_4O_2($^3\Sigma_g^-$) agrees well with the PES value.

Conclusion

In the present theoretical study, thermochemical properties of the small boron (B_n) and boron oxide (B_nO_m, with $n = 1-4$ and $m = 1-3$) clusters and their anions, as well as the B_4^{2-} dianion, were calculated by using coupled-cluster theory (U)CCSD(T) calculations with the aug-cc-pVnZ (n = D, T, Q, 5) basis sets extrapolated to the complete basis set limit with additional corrections. We predicted a uniform set of thermochemical parameters including enthalpies of formation, singlet−triplet or doublet−quartet separation gaps, bond dissociation energies, electron affinities, and vertical attachment and detachment energies. From our recent extensive studies on similar organic compounds, these calculated results are expected to be accurate to ±1.0 kcal/mol. In most cases, the new calculated

heats of formation show a fair agreement within experimental error bars of literature results. Our calculated electron affinities agree better with recent experimental results. There is no linearly additive relationship between thermochemical parameters with the number of B atoms. The calculated EAs of the boron oxides show considerable ability to capture electrons. For the structures studied, there is no relationship between the EA with the number of B atoms. For a fixed number of B atoms, the EA is, uniformly but not linearly, enhanced in going from the monoxide to the dioxide.

The thermodynamic results can be used to explain the growth mechanism of small boron oxide clusters B_nO_m. The strong B═O bond means that there is a predominant preference for formation of BO bonds just as in the transition metal oxide clusters $(MO_2)_n$ and $(MO_3)_n$ for group 4B and 6B metals where μ-oxo bonds are maintained as much as possible. Where possible, formation of a B_3 or B_4 cycle is also favored. The best combination arises when both a boron cycle and a BO bond can be simultaneously formed, as in the case of B_4O. When these factors compete with each other, the strong BO bonds compensate the destabilization arising from a loss of the intrinsic cyclic form of boron clusters, in such a way that a linear boron oxide prevails. The oxide derivative prefers a high spin state with a linear structure in which a distinct B_2 unit is preserved.

Acknowledgment. Funding was provided in part by the Department of Energy, Office of Energy Efficiency and Renewable Energy under the Hydrogen Storage Grand Challenge, Solicitation No. DE-PS36-03GO93013. This work was done as part of the Chemical Hydrogen Storage Center. D.A.D. is indebted to the Robert Ramsay Endowment of the University of Alabama. M.T.N. thanks the Flemish Fund for Scientific Research (FWO-Vlaanderen) and KULeuven Research Council for support. V.T.N. thanks the Vietnam Ministry for Education for a scholarship (program 322). We are grateful to the Alabama Supercomputing Center at Huntsville and the University of Alabama High Performance Computing Center for generous allocation of computer times.

Supporting Information Available: Total CCSD(T) electronic energies as a function of basis set extrapolated to the complete basis set limit. B_nO_m optimized structures at the CCSD(T) level of theory as a function of basis set. Calculated vibrational modes. Electronic energies for the electron affinities as a function of the basis set. Energy components and heats of formation of the lowest singlet and triplet state of BH_2^-. Figure of ELF isosurfaces of boron oxides with four boron atoms. This material is available free of charge via the Internet at http://pubs.acs.org.

References and Notes

(1) Lipscomb, W. N. *Boron Hydrides*; W. A. Benjamin: New York, 1963.

(2) Muetterties, E. L., Ed. *Boron Hydride Chemistry*; Academic Press: New York, 1975.

(3) (a) Liebman, J. F., Greenberg, A., Williams, R. E., Eds. *Advances in Boron and Boranes*; VCH Publishers: New York, 1988. (b) Siebert, W., Ed. *Advances in Boron Chemistry*; The Royal Society of Chemistry: Cambridge, UK, 1997.

(4) (a) Feath, G. M. *Prog. Energy Combust. Sci.* **1983**, *9*, 1. (b) Meinkohn, D. *Combust. Flame* **1985**, *59*, 225.

(5) (a) Slattery, D. K.; Hampton, M. D. Proceedings of the 2002 U.S. DOE Hydrogen Program Review. NREL/CP-610-32405. (b) Dressalhaus, M.; Crabtree, G.; Buchanan, M. Basic Energy Needs for the Hydrogen Economy. *Basic Energy Sciences*; Office of Science, U.S. Department of Energy: Washington, DC, 2003. (c) Ramage, M. P. *The Hydrogen Economy: Opportunities, Costs, Barriers, and R&D Needs*; The National Academies Press: Washington, DC, 2004.

(6) Stephens, F. H.; Pons, V.; Baker, R. T. *Dalton Trans.* **2007**, 2613.

(7) Alexandrova, A. N.; Boldyrev, A. I.; Zhai, H. J.; Wang, L. S. *Coord. Chem. Rev.* **2006**, *250*, 2811.

(8) Quandt, A.; Boustani, I. *ChemPhysChem* **2006**, *6*, 2001.

(9) (a) Gopukumar, G.; Nguyen, M. T.; Ceulemans, A. *Chem. Phys. Lett.* **2008**, *450*, 175. (b) Ceulemans, A.; Tshishimbi Muya, J.; Gopukumar, G.; Nguyen, M. T. *Chem. Phys. Lett.* **2008**, *461*, 226.

(10) Doyle, R. J. *J. Am. Chem. Soc.* **1988**, *110*, 4120.

(11) (a) Hintz, P. A.; Ruatta, S. A.; Anderson, S. L. *J. Chem. Phys.* **1990**, *92*, 292. (b) Hanley, L.; Anderson, S. L. *J. Chem. Phys.* **1988**, *89*, 2848. (c) Hintz, P. A.; Ruatta, S. A.; Anderson, S. L. *J. Chem. Phys.* **1991**, *94*, 6446. (d) Smolanoff, J.; Lapicki, A.; Kline, N.; Anderson, S. L. *J. Phys. Chem.* **1995**, *99*, 16276. (e) Peiris, D.; Lapicki, A.; Anderson, S. L.; Napora, R.; Linder, D.; Page, M. *J. Phys. Chem. A* **1997**, *101*, 9935. (f) Lapicki, A.; Peiris, D.; Anderson, S. L. *J. Phys. Chem. A* **1999**, *103*, 226.

(12) Tanimoto, M.; Saito, S.; Hirota, E. *J. Chem. Phys.* **1986**, *84*, 1210.

(13) Burkholder, T. R.; Andrews, L. *J. Chem. Phys.* **1991**, *95*, 8697.

(14) Maki, A. G.; Burkholder, J. B.; Sinha, A.; Howard, C. J. *J. Mol. Spectrosc.* **1988**, *130*, 238.

(15) Gong, Y.; Zhou, M. *J. Phys. Chem. A* **2008**, *112*, 5670.

(16) (a) Green, G. J.; Gole, J. L. *Chem. Phys. Lett.* **1980**, *69*, 45. (b) Gole, J. L.; Ohllson, B.; Green, G. *Chem. Phys.* **2001**, *273*, 59.

(17) Bullitt, M. K.; Paladugu, R. R.; DeHaven, J.; Davidovits, P. *J. Phys. Chem.* **1984**, *88*, 4542.

(18) Russell, D. K.; Kroll, M.; Beaudet, R. A. *J. Chem. Phys.* **1977**, *66*, 1999.

(19) Kawaguchi, K.; Hirota, E. *J. Mol. Spectrosc.* **1986**, *116*, 450.

(20) Adam, A. G.; Merer, A. J.; Steunenberg, D. M. *J. Chem. Phys.* **1990**, *92*, 2848.

(21) Ruscic, B. M.; Curtiss, L. A.; Berkowitz, J. *J. Chem. Phys.* **1984**, *80*, 3962.

(22) Wenthold, P. G.; Kim, J. B.; Jonas, K. L.; Lineberger, W. C. *J. Phys. Chem. A* **1997**, *101*, 4472.

(23) (a) Zhai, H. J.; Wang, L. M.; Li, S. D.; Wang, L. S. *J. Phys. Chem. A* **2007**, *111*, 1030. (b) Zhai, H. J.; Li, S. D.; Wang, L. S. *J. Am. Chem. Soc.* **2007**, *129*, 9254. (c) Li, S. D.; Zhai, H. J.; Wang, L. S. *J. Am. Chem. Soc.* **2008**, *130*, 2753.

(24) Nguyen, M. T.; Ruelle, P.; Ha, T. K. *J. Mol. Struct. (THEOCHEM)* **1983**, *104*, 353, and references therein.

(25) Nguyen, M. T. *Mol. Phys.* **1986**, *58*, 655.

(26) Gupta, A.; Tossell, J. A. *Am. Mineral.* **1983**, *68*, 989.

(27) Mains, G. J. *J. Phys. Chem.* **1991**, *95*, 5089.

(28) Martin, J. M. L.; Francois, J. P.; Gijbels, R. *Chem. Phys. Lett.* **1992**, *193*, 243.

(29) Brommer, M.; Rosmus, P. *J. Chem. Phys.* **1993**, *98*, 7746.

(30) Ortiz, J. V. *J. Chem. Phys.* **1993**, *99*, 6727.

(31) Neumukhin, A. V.; Weinhold, F. *J. Chem. Phys.* **1993**, *98*, 1329.

(32) Neumukhin, A. V.; Serebrennikov, L. V. *Russ. Chem. Rev.* **1993**, *62*, 527.

(33) Chen, K.; Lee, K.; Chang, J.; Sung, C.; Chung, T.; Liu, T.; Perng, H. *J. Phys. Chem.* **1996**, *100*, 488.

(34) Papakondylis, A.; Mavridis, A. *J. Phys. Chem. A* **1999**, *103*, 9359.

(35) (a) Grein, F. *J. Phys. Chem. A* **2005**, *109*, 9270. (b) Grein, F. *Chem. Phys. Lett.* **2006**, *418*, 100.

(36) Islam, M. M.; Bredow, T.; Minot, C. *Chem. Phys. Lett.* **2006**, *418*, 565.

(37) Liakoc, D. G.; Simandiras, E. D. *J. Phys. Chem. A* **2008**, *112*, 7881.

(38) Chin, C. H.; Mebel, A. M.; Hwang, D. Y. *J. Phys. Chem. A* **2004**, *108*, 473.

(39) Drummond, M. L.; Meunier, V.; Sumpter, B. G. *J. Phys. Chem. A* **2007**, *111*, 6539.

(40) Zhan, C. G.; Zheng, F.; Dixon, D. A. *J. Am. Chem. Soc.* **2002**, *124*, 14795.

(41) (a) Feller, D.; Dixon, D. A.; Peterson, K. A. *J. Phys. Chem. A* **1998**, *102*, 7053. (b) Dixon, D. A.; Gutowski, M. *J. Phys. Chem. A* **2005**, *109*, 5129. (c) Grant, D. J.; Dixon, D. A. *J. Phys. Chem. A* **2005**, *109*, 10138. (d) Grant, D. J.; Dixon, D. A. *J. Phys. Chem. A* **2006**, *110*, 12955.

(42) (a) Nguyen, M. T.; Nguyen, V. S.; Matus, M. H.; Gopakumar, G.; Dixon, D. A. *J. Phys. Chem. A* **2007**, *111*, 679. (b) Nguyen, V. S.; Matus, M. H.; Grant, D. J.; Nguyen, M. T.; Dixon, D. A. *J. Phys. Chem. A* **2007**, *111*, 8844. (c) Nguyen, V. S.; Matus, M. H.; Nguyen, M. T.; Dixon, D. A. *J. Phys. Chem. C* **2007**, *111*, 9603. (d) Nguyen, M. T.; Matus, M. H.; Dixon, D. A. *Inorg. Chem.* **2007**, *46*, 7561.

(43) (a) Stephens, F. H.; Baker, R. T.; Matus, M. H.; Grant, D. J.; Dixon, D. A. *Angew. Chem.* **2007**, *119*, 649; *Angew. Chem., Int. Ed.* **2007**, *46*, 641. (b) Matus, M. H.; Anderson, K. D.; Camaioni, D. M.; Autrey, S. T.; Dixon, D. A. *J. Phys. Chem. A* **2007**, *111*, 4411.

(44) Frisch, M. J.; Trucks, G. W.; Schlegel, H. B.; Scuseria, G. E.; Robb, M. A.; Cheeseman, J. R.; Montgomery, J. A., Jr.; Vreven, T.; Kudin, K. N.; Burant, J. C.; Millam, J. M.; Iyengar, S. S.; Tomasi, J.; Barone, V.; Mennucci, B.; Cossi, M.; Scalmani, G.; Rega, N.; Petersson, G. A.; Nakatsuji, H.; Hada, M.; Ehara, M.; Toyota, K.; Fukuda, R.; Hasegawa, J.;

Ishida, M.; Nakajima, T.; Honda, Y.; Kitao, O.; Nakai, H.; Klene, M.; Li, X.; Knox, J. E.; Hratchian, H. P.; Cross, J. B.; Bakken, V.; Adamo, C.; Jaramillo, J.; Gomperts, R.; Stratmann, R. E.; Yazyev, O.; Austin, A. J.; Cammi, R.; Pomelli, C.; Ochterski, J. W.; Ayala, P. Y.; Morokuma, K.; Voth, G. A.; Salvador, P.; Dannenberg, J. J.; Zakrzewski, V. G.; Dapprich, S.; Daniels, A. D.; Strain, M. C.; Farkas, O.; Malick, D. K.; Rabuck, A. D.; Raghavachari, K.; Foresman, J. B.; Ortiz, J. V.; Cui, Q.; Baboul, A. G.; Clifford, S.; Cioslowski, J.; Stefanov, B. B.; Liu, G.; Liashenko, A.; Piskorz, P.; Komaromi, I.; Martin, R. L.; Fox, D. J.; Keith, T.; Al-Laham, M. A.; Peng, C. Y.; Nanayakkara, A.; Challacombe, M.; Gill, P. M. W.; Johnson, B.; Chen, W.; Wong, M. W.; Gonzalez, C.; Pople, J. A. *Gaussian 03*, revision C.01; Gaussian, Inc.: Wallingford, CT, 2004.

(45) Werner, H.-J.; Knowles, P. J.; Amos, R. D.; Bernhardsson, A.; Berning, A.; Celani, P.; Cooper, D. L.; Deegan, M. J. O.; Dobbyn, A. J.; Eckert, F.; Hampel, C.; Hetzer, G.; Korona, T.; Lindh, R.; Lloyd, A. W.; McNicholas, S. J.; Manby, F. R.; Meyer, W.; Mura, M. E.; Nicklass, A.; Palmieri, P.; Pitzer, R. M.; Rauhut, G.; Schütz, M.; Stoll, H.; Stone, A. J.; Tarroni, R.; Thorsteinsson, T. *MOLPRO-2002, a package of initio programs*; Universität Stüttgart, Stüttgart, Germany; University of Birmingham, Birmingham, UK, 2002.

(46) (a) Peterson, K. A.; Xantheas, S. S.; Dixon, D. A.; Dunning, T. H., Jr. *J. Phys. Chem. A* **1998**, *102*, 2449. (b) Feller, D.; Peterson, K. A. *J. Chem. Phys.* **1998**, *108*, 154. (c) Dixon, D. A.; Feller, D. *J. Phys. Chem. A* **1998**, *102*, 8209. (d) Feller, D.; Peterson, K. A. *J. Chem. Phys.* **1999**, *110*, 8384. (e) Feller, D.; Dixon, D. A. *J. Phys. Chem. A* **1999**, *103*, 6413. (f) Feller, D. *J. Chem. Phys.* **1999**, *111*, 4373. (g) Feller, D.; Dixon, D. A. *J. Phys. Chem. A* **2000**, *104*, 3048. (h) Feller, D.; Sordo, J. A. *J. Chem. Phys.* **2000**, *113*, 485. (i) Feller, D.; Dixon, D. A. *J. Chem. Phys.* **2001**, *115*, 3484. (j) Dixon, D. A.; Feller, D.; Sandrone, G. *J. Phys. Chem. A* **1999**, *103*, 4744. (k) Ruscic, B.; Wagner, A. F.; Harding, L. B.; Asher, R. L.; Feller, D.; Dixon, D. A.; Peterson, K. A.; Song, Y.; Qian, X.; Ng, C.; Liu, J.; Chen, W.; Schwenke, D. W. *J. Phys. Chem. A* **2002**, *106*, 2727. (l) Feller, D.; Dixon, D. A.; Peterson, K. A. *J. Phys. Chem. A* **1998**, *102*, 7053. (m) Dixon, D. A.; Feller, D.; Peterson, K. A. *J. Chem. Phys.* **2001**, *115*, 2576.

(47) Bartlett, R. J.; Musial, M. *Rev. Mod. Phys.* **2007**, *79*, 291, and references therein.

(48) (a) Dunning, T. H. *J. Chem. Phys.* **1989**, *90*, 1007. (b) Kendell, R. A.; Dunning, T. H.; Harrison, R. J. *J. Chem. Phys.* **1992**, *96*, 6796.

(49) Rittby, M.; Bartlett, R. J. *J. Phys. Chem.* **1988**, *92*, 3033.

(50) Knowles, P. J.; Hampel, C.; Werner, H.-J. *J. Chem. Phys.* **1994**, *99*, 5219.

(51) Deegan, M. J. O.; Knowles, P. J. *Chem. Phys. Lett.* **1994**, *227*, 321.

(52) Peterson, K. A.; Woon, D. E.; Dunning, T. H., Jr. *J. Chem. Phys.* **1994**, *100*, 7410.

(53) (a) Peterson, K. A.; Dunning, T. H., Jr. *J. Chem. Phys.* **2002**, *117*, 10548. (b) Woon, D. E.; Dunning, T. H., Jr. *J. Chem. Phys.* **1993**, *98*, 1358.

(54) Dunham, J. L. *Phys. Rev.* **1932**, *41*, 713.

(55) (a) Helgaker, T.; Klopper, W.; Koch, H.; Nagel, J. *J. Chem. Phys.* **1997**, *106*, 9639. (b) Halkier, A.; Helgaker, T.; Jørgensen, P.; Klopper, W.; Koch, H.; Olsen, J.; Wilson, A. K. *Chem. Phys. Lett.* **1998**, *286*, 243.

(56) (a) Douglas, M.; Kroll, N. M. *Ann. Phys.* **1974**, *82*, 89–155. (b) Hess, B. A. *Phys. Rev. A* **1985**, *32*, 756–763. (c) Hess, B. A. *Phys. Rev. A* **1986**, *33*, 3742–3748.

(57) de Jong, W. A.; Harrison, R. J.; Dixon, D. A. *J. Chem. Phys.* **2001**, *114*, 48.

(58) EMSL basis set library. http://www.emsl.pnl.gov/forms/basisform.html.

(59) Moore, C. E. Atomic energy levels as derived from the analysis of optical spectra, Volume 1, H to V; *U.S. National Bureau of Standards Circular 467*; U.S. Department of Commerce, National Technical Information Service, COM-72-50282: Washington, DC, 1949.

(60) Karton, A.; Martin, J. M. L. *J. Phys. Chem. A* **2007**, *111*, 5936.

(61) Chase, M. W. *J. Phys. Chem. Ref. Data, Monogr.* **1998**, *9* (Suppl. 1), 1–957.

(62) Storms, E.; Mueller, B. *J. Phys. Chem.* **1977**, *81*, 318.

(63) Ruscic, B.; Mayhew, C. A.; Berkowitz, J. *J. Chem. Phys.* **1988**, *88*, 5580.

(64) Martin, J. M. L.; Taylor, P. R. *J. Phys. Chem. A* **1998**, *102*, 2995.

(65) Cox, J. D.; Wagman, D. D.; Medvedev, V. A. *CODATA Key Values for Thermodynamics*; Hemisphere Publishing Corp.: New York, 1989.

(66) Gurvich, L. V.; Veyts, I. V.; Alcock, C. B. *Thermodynamic Properties of Individual Substances*; Begell House: New York, 1996; Vol. 3.

(67) Curtiss, L. A.; Raghavachari, K.; Redfern, P. C.; Pople, J. A. *J. Chem. Phys.* **1997**, *106*, 1063.

(68) Douglas, A. E.; Herzberg, G. *Can. J. Res. A* **1940**, *18*, 165.

(69) Deutsch, P. W.; Curtius, L. A.; Pople, J. A. *Chem. Phys. Lett.* **1990**, *174*, 33.

(70) Martin, J. M. L.; Francois, J. P.; Gijbels, R. *Chem. Phys. Lett.* **1992**, *189*, 529.

(71) Langhoff, S. R.; Bauschlicher, C. W., Jr. *J. Chem. Phys.* **1991**, *95*, 5882.

(72) Huber, K. P.; Herzberg, G. *Molecular Spectra and Molecular Structure IV. Constants of Diatomic Molecules*; Van Nostrand: New York, 1979.

(73) Verhaegen, D. *J. Chem. Phys.* **1962**, *37*, 1367, and ref 60 for heat of formation of B.

(74) Bruna, P. J.; Wright, J. S. *J. Phys. Chem.* **1990**, *94*, 1774.

(75) Reid, C. J. *Int. J. Mass Spectrom. Ion Processes* **1993**, *127*, 147.

(76) Takeuchi, T.; Yamamoto, M.; Kiuchi, M. *Nucl. Instrum. Methods Phys. Res., Sect. B* **1999**, *153*, 298.

(77) NIST Chemistry Webbook: http://webbook.nist.gov.

(78) Scheer, M.; Bilodeau, R. C.; Haugen, H. K. *Phys. Rev. Lett.* **1998**, *80*, 2562.

(79) Cias, P.; Araki, M.; Denisov, A.; Maier, J. P. *J. Chem. Phys.* **2004**, *121*, 6776.

(80) Zhai, H.-J.; Wang, L.-S.; Alexandrova, A. N.; Boldyrev, A. I.; Zakrzewski, V. G. *J. Phys. Chem. A* **2003**, *107*, 9319.

(81) Li, S.; Van Zee, R. J.; Weltner, W., Jr. *Chem. Phys. Lett.* **1996**, *262*, 298.

(82) Lee, T. J.; Taylor, P. R. *Int. J. Quantum Chem.* **1989**, *S23*, 199.

(83) Hernandez, R.; Simons, J. *J. Chem. Phys.* **1991**, *94*, 2691.

(84) Zhai, H. J.; Wang, L. S.; Alenxandrova, A. N.; Boldyrev, A. I.; Zakrzewski, V. G. *J. Phys. Chem. A* **2003**, *107*, 9319.

(85) Venkatesan, T. S.; Deepika, K.; Mahapatra, S. *J. Comput. Chem.* **2006**, *27*, 1093.

(86) Zubarev, D. Yu.; Boldyrev, A. I. *J. Comput. Chem.* **2006**, *28*, 251.

(87) (a) Becke, A. D.; Edgecombe, K. E. *J. Chem. Phys.* **1990**, *92*, 5397. (b) Silvi, B.; Savin, A. *Nature* **1994**, *371*, 63.

(88) Nguyen, M. T.; Nguyen, V. S.; Matus, M. H.; Gopakumar, G.; Dixon, D. A. *J. Phys. Chem. A* **2007**, *111*, 679.

(89) Dewar, M. J. S.; Del Lano, C. *J. Am. Chem. Soc.* **1969**, *91*, 789.

(90) Kato, H.; Tanaka, E. *J. Comput. Chem.* **1991**, *12*, 1097.

(91) Kato, H.; Yamashita, K.; Morokuma, K. *Chem. Phys. Lett.* **1992**, *190*, 361.

(92) Ray, A. K.; Howard, I. A.; Kanal, K. M. *Phys. Rev. B* **1992**, *45*, 14247.

(93) (a) Boustani, I. *Chem. Phys. Lett.* **1995**, *240*, 135. (b) Boustani, I. *Chem. Phys. Lett.* **1995**, *233*, 273.

(94) Abdurahman, A.; Shukla, A.; Seifert, G. *Phys. Rev. B* **2002**, *66*, 155423.

(95) Jin, H. W.; Li, Q. S. *Phys. Chem. Chem. Phys.* **2003**, *5*, 1110.

(96) Linguerri, R.; Navizet, I.; Rosmus, P.; Carter, S.; Maier, J. P. *J. Chem. Phys.* **2005**, *122*, 034301.

(97) Atis, M.; Özdogan, C.; Güvenc, Z. B. *Int. J. Quantum Chem.* **2007**, *107*, 729.

(98) Juselius, J.; Straka, M.; Sundholm, D. *J. Phys. Chem. A* **2001**, *105*, 9939.

(99) Lambrecht, D. S.; Fleig, T.; Sommerfeld, T. *J. Phys. Chem. A* **2008**, *112*, 2855–7986.

(100) Zubarev, D. Yu.; Boldyrev, A. I. *J. Phys. Chem. A* **2008**, *112*, 7984.

(101) Cyranski, M. K. *Chem. Rev.* **2005**, *105*, 3773.

(102) Feng, X. J.; Luo, Y. H. *J. Phys. Chem. A* **2007**, *111*, 2420.

(103) Jiang, Z. Y.; Yang, C. J.; Li, S. T. *J. Chem. Phys.* **2005**, *123*, 204315.

(104) Jensen, D. E. *J. Chem. Phys.* **1970**, *52*, 3305.

(105) Srivastava, R. D.; Uy, O. M.; Farber, M. *Trans. Faraday Soc.* **1971**, *67*, 2941.

(106) Harmony, M. D.; Laurie, V. W.; Kuczkowski, R. L.; Schwendeman, R. H.; Ramsey, D. A.; Lovas, F. J.; Lafferty, W. J.; Maki, A. G. *J. Phys. Chem. Ref. Data* **1979**, *8*, 619.

(107) Kuchitsu, K., Ed. *Structure of Free Polyatomic Molecules - Basic Data*; Springer: Berlin, 1998.

(108) Johns, J. W. C. *Can. J. Phys* **1961**, *39*, 1738.

(109) Kawaguchi, K.; Hirota, H.; Yamada, C. *Mol. Phys.* **1981**, *44*, 509.

(110) Semenikin, V. I.; Minaeva, I. I.; Sorokin, I. D.; Nikitin, M. I.; Rudnyi, E. B.; Sidorov, L. N. *High Temp. Phys. (Engl.)* **1987**, *25*, 49.

(111) Nguyen, M. T. *J. Mol. Struct. (THEOCHEM)* **1986**, *136*, 371.

(112) Sidorov, L. N.; Rudnyi, E. B.; Nikitin, M. I.; Sorokin, I. D. *Dokl. Akad. Nauk SSSR Ser. Khim.* **1983**, *272*, 1172.

(113) Inghram, M. G.; Porter, R. F.; Chupka, W. A. *J. Chem. Phys.* **1956**, *25*, 498.

(114) Maloney, K. M.; Gupta, S. G.; Lynch, D. A. *J. Inorg. Nucl. Chem.* **1976**, *38*, 2163.

(115) DeKock, R. L.; Barbachyn, M. R. *J. Inorg. Nucl. Chem.* **1981**, *43*, 2465.

(116) Graham, W. R.; Weltner, W., Jr. *J. Chem. Phys.* **1976**, *65*, 1576.

(117) (a) Sekachev, Y. N.; Serebrennikov, L. V.; Mal'tsev, A. A. *Vestnik. Mosk. Univ. Khim.* **1979**, *20*, 589. (b) Serebrennikov, L. V. *Vestnik. Mosk. Univ. Khim.* **1981**, *22*, 606.

(118) (a) Chawla, N.; Kerr, M.; Chawla, K. K. *J. Am. Ceram. Soc.* **2005**, *88*, 101. (b) Indris, S.; Heitjans, P.; Roman, H.; Bunde, A. *Phys. Rev. Lett.* **2000**, *84*, 2889.

(119) Weltner, W., Jr.; Warn, J. R. W. *J. Chem. Phys.* **1962**, *37*, 292.

(120) Nguyen, M. T.; Ruelle, P.; Ha, T. K. *J. Mol. Struct. (THEOCHEM)* **1983**, *104*, 353, and references therein.

(121) Jemmis, E. D.; Giju, K. T.; Leszczynski, J. *Electron. J. Theor. Chem.* **1997**, *2*, 130.

(122) Gu, J.-P.; Buenker, R. J.; Hirsch, G.; Jensen, P.; Bunker, P. R. *J. Mol. Spectrosc.* **1996**, *178*, 172.

(123) (a) Leopold, D. G.; Murray, K. K.; Miller, A. E. S.; Lineberger, W. C. *J. Chem. Phys.* **1985**, *83*, 4849. (b) Bunker, P. R.; Sears, T. J. *J. Chem. Phys.* **1985**, *83*, 4866. (c) Khan, M. I.; Goodman, J. L. *J. Am. Chem. Soc.* **1995**, *117*, 6635. (d) Ruscic, B.; Litorja, M.; Asher, R. L. *J. Phys. Chem. A* **1999**, *103*, 8625.

(124) Sander, S. P.; Friedl, R. R.; Ravishankara, A. R.; Golden, D. M.; Kolb, C. E.; Kurylo, M. J.; Huie, R. E.; Orkin, V. L.; Molina, M. J.; Moortgat, G. K.; Finlayson-Pitts, B. J. Chemical Kinetics and Photochemical Data for Use in Atmospheric Studies: Evaluation Number 14; *JPL Publication 02-25, National Aeronautics and Space Administration*; Jet Propulsion Laboratory, California Institute of Technology: Pasadena, CA, 2003; http://jpldataeval.jpl.nasa.gov/pdf/JPL_02-25_rev02.pdf.

JP811391V